Die ökologische Rolle von Glukosinolate als Pflanzenabwehrstoffe:

Ihre Wirksamkeit gegen Generalisten– und Spezialisten–Herbivoren

Dissertation

zur Erlangung des akademischen Grades doctor rerum naturalium (Dr. rer. nat.)

Vorgelegt dem Rat der Biologisch–Pharmazeutischen Fakultät

der Friedrich–Schiller–Universität Jena

Von Master in Science

Luis Fredd Leonardo Vergara Montalvo

geboren am 6. November 1976 in Otumba, México

1. Table of contents

Strangers passing in the street

by chance two separate glances meet

and I am you and what I see is me.

Foreword

Back in the late 90s I was an undergraduate science student of in Mexico City. When the time to plan what to do during the summer break came I had always the same list of priorities: My girlfriend, football, getting a two– to three–weeks job and taking part in one of the many summer science projects offered in flyers on the walls of the administrative zone of the faculty building. These were my first practical experiences with science and they did nothing but deepened my love for it. I had neither before manipulated state of the art equipment for analytical chemistry and became fascinated with the complexity and beauty of objects I could just imagine but not see with my eyes. I had never before understood the complexity and beauty of the living world before it was revealed to me luxuriantly in the form of the tropical rainforest where I assisted in field ecology projects. These were the gametes of an intimate symbiont that fused its genes with mine and whispered to me at night that I had chosen the best of all fates possible, thus transforming me into the student of science I am today.

As this thesis will attest, chemistry and biology are omnipresent parts of my life, but they are no longer individual entities. They have evolved into a hybrid known as chemical ecology which has become my chosen field of endeavour.

Promotionskomission

Gutachter

1. Prof. Dr. Jonathan Gershenzon.

2. Prof. Dr. David Heckel.

3. Prof. Dr. Caroline Müller.

Tag der öffentlichen Verteidigung: 21.10.2008.

2. Manuscript Summaries

Manuskript I

Glycine Conjugates in a Lepidopteran Insect Herbivore–The Metabolism of Benzylglucosinolate in the Cabbage White Butterfly, *Pieris rapae*

Pieris rapae, der Kleine Kohlweißling, ernährt sich von Brassicaceae–Pflanzen (z. B. Brokkoli, Kohl, Raps, Senf), die Glukosinolate sowie Myrosinasen produzieren. Die Glukosinolate sind eine Gruppe von Naturstoffen mit einheitlicher schwefelhaltiger Grundstruktur, aber variablen Seitenketten wie aliphatischen Kohlenwasserstoffketten und Aromaten sowie Kombinationen von beiden. Wenn die Raupen die Pflanzen fressen, hydrolysiert die Myrosinase die Glukosinolate, und als Produkte entstehen Isothiocyanate. Die Isothiocyanate sind vermutlich giftig für viele Insekten, aber *P. rapae* produziert ein Protein (NSP), das die Hydrolyse der Glukosinolate dahingehend beeinflußt, dass Nitrile statt Isothiocyanaten produziert werden. Die Toxizität der Nitrile ist vermutlich geringer als die von Isothiocyanaten, dadurch kann *P. rapae* Brassicaceae–Pflanzen fressen. Während Nitrile von verschiedenen Glukosinolaten in den Fäzes der Raupen in vorherigen Studien gefunden wurden, wurde das Nitril von Benzylglukosinolat bisher nicht im Raupenkot entdeckt. Unsere Ergebnisse zeigen, dass das Nitril des Benzylglukosinolats im Darm der Raupe weiter umgewandelt und Hippursäure als Endprodukt produziert wird. Konjugierte Aminosäuren wie Hippursäure, das Reaktionsprodukt von Benzoesäure und Glycin, sind polare, hydrophile Subtanzen, weswegen die Raupe sie leichter ausscheiden kann. Da die Konzentration des Benzylglukosinolats in Pflanzen wie *Tropaeolum majus* (Kapuzinerkresse) sehr hoch ist, könnte die Fähigkeit der Konjugation des Abbauproduktes des Benzylglukosinolates mit Aminosäuren ein evolutionärer Vorteil für *P. rapae* sein, weil seine Raupen wenige konkurrierende Herbivoren in dieser ökologischen Nische haben. Damit zeigen diese Forschungsergebnisse zum ersten Mal das Wirkungsprinzip der Aminosäurekonjugation zur Entgiftung von Xenobiotica in Schmetterlingen.

Non-Uniform Distribution of Glucosinolates in *Arabidopsis thaliana*

Leaves has Important Consequences for Plant Defense

In „Pflanzen und Schnecken. Eine biologische Studie über die Schutzmittel der Pflanzen gegen Schneckenfraß (1888)" beschrieb Ernst Stahl, der Ende des 19. Jahrhunderts und Anfang des 20. Jahrhunderts an der Friedrich–Schiller–Universität Jena als Botaniker gearbeitet hat, folgende Beobachtungen in den Alpen: „In der Nähe der Sennhütten bleibt die gerbstoffreiche Alchemilla mit einigen wenigen andern Pflanzen völlig unangetastet. Andre Pflanzen, welche dem Heu einen angenehmen Geruch verleihen, und von welchen angenommen wird, daß sie anregend auf die Verdauung der Tiere wirken, bleiben auf den Triften meist unberührt… Ist einmal durch Versuche festgestellt, daß eine Tierart eine Pflanze oder einen *Pflanzenteil* gar nicht oder nur ungern verzehrt, so tritt die weitere Frage heran, warum dies der Fall ist".

Mehr als ein Jahrhundert später haben wir beobachtet, dass die ersten Raupenstadien des Baumwollkapselwurms (*Helicoverpa armigera*) nur diejenigen Blattbereiche der Acker–Schmalwand (*Arabidopsis thaliana*) fressen, die zwischen der Mittelrippe und dem Blattrand liegen. Wir können mit Hilfe der modernen Technik im Bereich der analytischen Chemie die genaue Lokalisierung der Glukosinolate in Blättern von *A. thaliana* durchführen und deren Wirksamkeit als Abwehrstoffe gegen *H. armigera* herausfinden. Mit Hilfe der durch Matrix–unterstützte Laser–Desorption/Ionisierung (MALDI)–Massenspektrometrie erzeugten Bildgebung der Hauptglukosinolate in Blättern von *A. thaliana* können wir zeigen, dass die Glukosinolate keine gleichmäßige Horizontalverteilung haben, sondern entlang der Mittelrippe und des Blattrandes konzentriert sind. Das entspricht genau den Bereichen des Blattes, die die jungen *H. armigera* Raupen nicht fressen wollen. Die Mittelrippe ist sehr wichtig für die Physiologie des Blattes und der Blattrand ist die erste Region, an der viele Pflanzenfresser ihren Angriff starten. Infolgedessen müssten diese zwei Zonen besonders gut verteidigt sein, d. h. eine hohe Konzentration von Glukosinolaten aufweissen, und damit die Möglichkeit haben, ihren Feinden zu widerstehen.

Die Entwicklung einer leistungsfähigen massenpektrometrischen Bildgebungstechnik ermöglichte es, die Komplexität der ökologischen

Wechselwirkungen zwischen Pflanzen und Pflanzenfressern in diesem Maßstab zu untersuchen und die phänomenologische Ähnlichkeit mit Stahls Hypothese zu erkennen, dass nämlich die Lokalisierung der Pflanzeninhaltsstoffe eine Pflanzeneigenschaft ist, die die Wechselwirkungen zwischen Pflanzen und Pflanzenfressern beeinflusst.

Manuskript III

Determination of the Absolute Configuration of the
Glucosinolate Methyl Sulfoxide Group
Reveals a Stereospecific Biosynthesis of the Side Chain

Glukosinolate (Senfölglykoside) sind sekundäre Pflanzeninhaltsstoffe, mit einer β–D–Thioglukopyranose als Kernstruktur. Sie werden von Pflanzen der Familie der Brassicaceae produziert und sind vermutlich inaktive Substanzen, jedoch produzieren die Brassicaceaen auch Myrosinasen, Enzyme, die die Glukosinolate nach Gewebezerstörung (z. B. nach einem Angriff durch Herbivoren) hydrolysieren. Die Hydrolyse–Produkte der Glukosinolate haben unterschiedliche biologische Wirkungen in der Natur, als abwehrende Substanzen gegen Pflanzenfresser und auch im medizinischen Bereich; z. B. wirkt das Produkt der Hydrolyse des Glukoraphanins (4–Methylsulfinylbutylglukosinolat) gegen einige Krebsarten. Trotz ihrer wichtigen biologischen Funktionen bleiben einige strukturelle Eigenschaften der Glukosinolate noch unbekannt. Glukoraphanin enthält ein Sulfoxid, eine funktionelle Gruppe, die ein unregelmäßiges Tetraeder als geometrische Struktur zeigt, weswegen das Schwefelatom chiral ist. Bisher gibt es keine Studie, die den Enantiomerenüberschuss sowie die absolute Konfiguration des Sulfoxids des Glukoraphanins erforscht hat. Unsere NMR–spektroskopischen Messungen mit chiralen lanthanoiden Verschiebungsreagenzien und intaktem Glukoraphanin bzw. mit seinem Moscher–Ester zeigen, dass das Sulfoxid des Glukoraphanins aus Brokkoli sowie aus *Arabidopsis thaliana* nur als ein Enantiomer vorliegt und die absolute Konfiguration R_S hat.

3. General Introduction

Living things are law breakers; they do not respect the second law of thermodynamics. To maintain themselves against the relentless force of entropy, they need to fuel their metabolic machinery with some kind of energy. Some have solved this problem by obtaining the energy they need from abiotic sources; some obtain it from other organisms. Food chains exist wherever we find living things. One very interesting link in these chains is herbivory, for plants are at the base of many food chains. The assemblage of plants in a particular area defines what we understand as ecosystems and consumption of plant tissues by herbivores can have a major impact on ecosystem structure. It has been estimated that over a million insect species feed on plants both above– and belowground using different feeding strategies. Approximately two thirds of all known herbivore insect species are leaf-eating beetles or caterpillars that cause damage chewing, snipping or tearing the leaves[5]. Unless plants receive something in return, they cannot tolerate excessive herbivory, for it could significantly reduce their reproductive fitness. Hence plants try to avoid or at least minimize the negative consequences of herbivory in different ways. The inverse situation applies for herbivores. They need to get access to the energy and nutrients locked in the form of plant organs or fluids and, in a biological chess game, they have evolutionarily explored different ways to reach this goal.

Understanding the chemical mechanisms developed by herbivores and plants to feed or avoid being eaten is the scope a vibrant branch of chemical ecology. As the main focus of my Ph. D. project, I have explored the molecular bases and the physiological consequences of some of these mechanisms using as a model of study the plant *Arabidopsis thaliana* and the caterpillars of two lepidopteran insects, *Pieris rapae* and *Helicoverpa armigera*.

Plant defense

The features expressed by plants to minimize herbivore feeding can be classified in different categories. Plant life histories can be shaped to germinate and grow during seasons when herbivore density is low, a mechanism known as temporal escape. Plant tissues can undergo toughening or hardening making them difficult to penetrate or masticate by herbivores, a mechanism known as mechanical defense. Finally, plant metabolism can produce substances that make plant tissues or fluids unpalatable or toxic to herbivores, a mechanism known as direct chemical defense. Such plant metabolites could also attract predators feeding on the attacking herbivores, a mechanism known as indirect defense. Plant defensive features are not mutually exclusive and one individual can express different mechanisms simultaneously.

Chemical defense

Plants produce an enormous range of chemical compounds that do not appear to have any role in the basic processes of growth and development. Once thought to be merely metabolic wastes and disdainfully referred to as *secondary metabolites* (a term that I completely dislike), this large group of plant compounds have been increasingly demonstrated to function in ecological interactions. In particular, the role of many plant metabolites as mediators of plant–herbivore interactions is now well supported both by experimental data. Many of these compounds are biosynthesized constitutively, whereas the production of others is triggered or induced, after herbivore feeding activity. Some of them act on a broad spectrum of herbivores, whereas others are active only against a small group of herbivores.
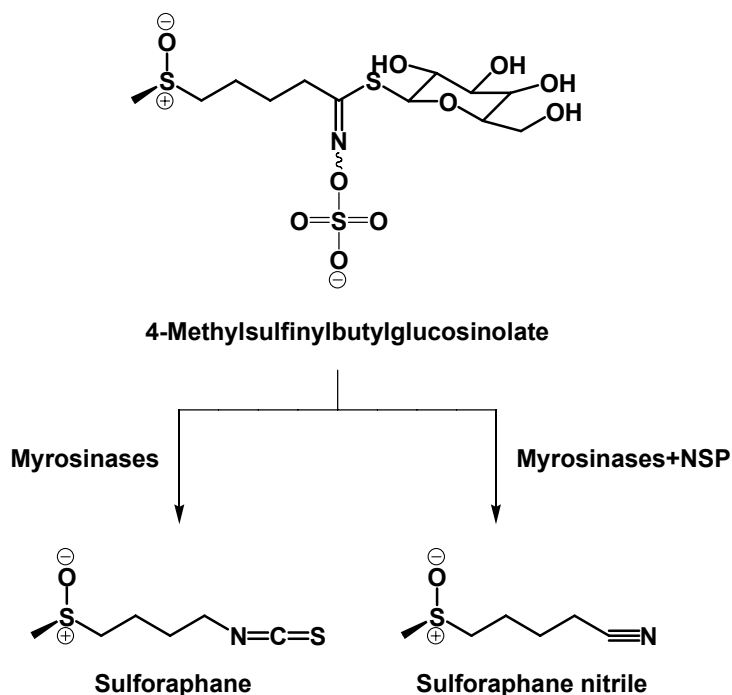
Glucosinolates

The structural diversity displayed by plant metabolites deserves additional discussion. Thousands of plant produced metabolites with vastly different chemical structures have been described. For practical reasons they are grouped into different families, some of them *natural*, *i. e.*, defined by a common biosynthetic origin, but others considered *artificial*, because their members do not share a common biosynthesis but rather a structural feature. Some of the main classes of plant metabolites in terms of numbers of compounds are: Isoprenoid compounds or

terpenoids; compounds derived from shikimate, like flavonoids, tannins and lignins; aliphatic compounds derived from serial condensation reactions of acetyl–CoA like fatty acids or polyketides; basic compounds containing nitrogen or alkaloids; glucosides and amino acids and small peptides and commonly plant metabolites are the result of combination of two or more families. The occurrence of these substances in the plant kingdom is heterogeneous; some metabolites are present in virtually any plant but others are circumscribed to a narrow taxonomical category. Glucosinolates are an example of plant metabolites of this last group, for they have been isolated almost exclusively from a single taxon, the Brassicales order[4]. Glucosinolates are biosynthesized constitutively and display a large structural diversity (Scheme 1) and currently more than 120 glucosinolates have been reported.

4-Methylsulfinylbutylglucosinolate   **Benzylglucosinolate**   **Indol-3-ylmethylglucosinolate**
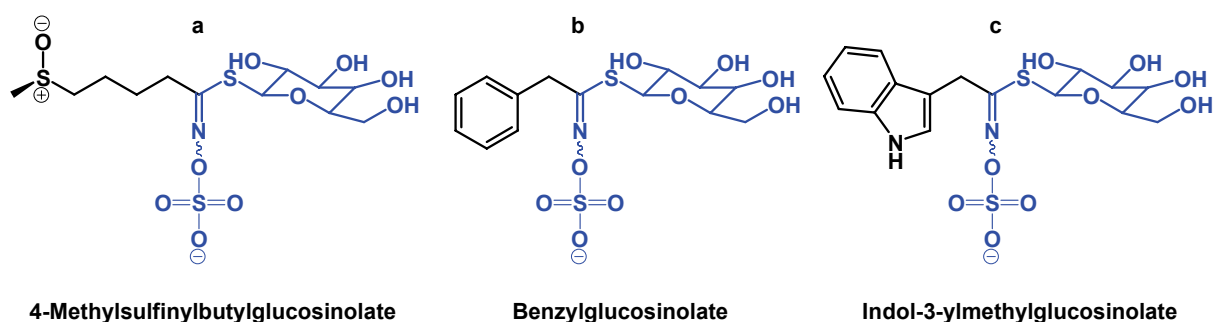
Scheme 1. Examples of subfamilies of glucosinolates isolated from Brassicales. (a) Aliphatic glucosinolate, (b) benzenoid glucosinolate and (c) indolic glucosinolate. The core structure defining a glucosinolate is highlighted in blue.

During the first half of the XIX century sulphur containing glucosides were first isolated from Brassicales plants and at the same time their connection with volatile mustard oils as a result of enzymatic hydrolytic activity was established[6]. After decades of research it is now well documented that glucosinolates are in principle biologically inert. But, when plant tissues are disrupted, for example after herbivore feeding activity, glucosinolates are activated by enzymes known as myrosinases to form hydrolysis products that have been shown to exert negative effects on the physiology of many classes of insect herbivores feeding on Brassicales[9] (Scheme 2).

Scheme 2. Enzymatic hydrolysis of glucosinolates. Myrosinases produce isothiocyanates from glucosinolates, but under the influence of NSP produced by *P. rapae* the products formed are nitriles.

Despite the presence of glucosinolate and myrosinases, many insect herbivores exploit plants of the Brassicales without any apparent negative consequences. How is this possible?

Insect offense

In spite of all the defensive features expressed by plants to avoid consumption of their tissues and fluids, herbivores manage to feed on protected plants. This is possible due to different mechanisms expressed by herbivores that nullify or minimize the action of plant defenses. For chemical defenses, these may be divided into behavioral and physiological mechanisms. Behavioral mechanisms comprise avoidance of high concentrations of chemical defenses or regulation of their uptake[2]. Physiological mechanisms include rapid excretion of plant metabolites, chemical modification (detoxification), sequestration and target site insensitivity. The presence or absence of these mechanisms ultimately determines whether an herbivore can exploit or not exploit a plant or part of a plant as food source. Evolution has

exquisitely tuned the metabolic machinery of some herbivores to counteract the action of defensive metabolites present in their diet. In some cases, this has led to a process of specialization, since the herbivore narrows its ecological niche to only a few host plants whose defense can be counteracted, *i. e.*, they become specialists or monophagous. At the opposite extreme, herbivores lacking such metabolic machinery can feed only on plants that are not well chemically protected. Herbivores that feed on a broad spectrum of plants, with or without counteradaptations, are called generalist or polyphagous.

Specialists of glucosinolate containing plants

One example of a specialist herbivore is *Pieris rapae*, the cabbage white butterfly, whose larval stages feed exclusively on Brassicales in nature[8]. Recently, a protein found in the gut of *P. rapae*, named the nitrile specifier protein (NSP), was suggested to be the molecular mechanism used by these caterpillars to tolerate glucosinolates[10]. In the presence of NSP, the myrosinases are no longer capable of transforming glucosinolates into isothiocyanates, toxic hydrolysis products thought to cause noxious effects on insects. Instead, glucosinolate hydrolysis is diverted to form nitriles, compounds thought to be much less toxic than isothiocyanates (Scheme 2).

The host range of *P. rapae* comprises many members of the Brassicales with varying glucosinolate profiles. One of these hosts is *Tropaeolum majus* (nasturtium or *Kapuzinerkresse*), which produces benzylglucosinolate[7]. Interestingly, the nitriles produced from different types glucosinolates were identified in feces of *P. rapae* and isolated NSP was shown to be able to influence the hydrolysis of many types of glucosinolate *in vitro*, including benzylglucosinolate, producing the corresponding nitriles. However, the nitrile of benzylglucosinolate was not detected after feeding *P. rapae* on benzylglucosinolate containing plants. This observation raised the question whether the compound was never formed, missed in analysis, or formed but then converted to another metabolite. In the course of this thesis work, a novel detoxification mechanism acting on the nitrile product of benzylglucosinolate hydrolysis was discovered which turned out to be the reason for the absence of this nitrile in feces extracts (see chapter 2.1).

Generalists of glucosinolate containing plants

Not all insects can exploit glucosinolate–myrosinase containing plants as efficiently as *P. rapae*. Insect herbivores that are not specialized on Brassicales can experience problems because of the presence of glucosinolate hydrolysis products in their diet. One case that exemplifies this situation is the polyphagous insect *H. armigera*, the cotton bollworm, whose larvae have been recorded on large number of hosts on the field, including members of the Brassicales. However, in a choice experiment performed under laboratory conditions they ranked the plants offered to them into the following hierarchy: Tobacco, maize, sunflower and cabbage[3]. This information suggests that, although these larva can feed on glucosinolate-myrosinase containing plants they do not find these plants very palatable making this a very attractive model for comparing the physiology of specialists *versus* generalist insects feeding on Brassicales in terms of their response to glucosinolates as chemical defenses.

As part of this thesis, experiments were conducted in which *H. armigera* larvae were fed either with the *A. thaliana* accession Columbia–0 (*A. thaliana* Col–0) or with the transgenic *A. thaliana tgg1*/*tgg2* (a line developed from an *A. thaliana* Col–0 background), a genotype differing from the wild–type Col–0 exclusively in the mutation of the two myrosinase encoding genes expressed in leaves, and therefore being unable to hydrolyze glucosinolates[1]. Using these lines, it was found that the weight gain of *H. armigera* at 10 days after hatching was three times higher with the *A. thaliana tgg1*/*tgg2* plants than with Col–0. Remarkably, the first instars displayed a contrasting feeding activity on the two lines. Whereas larvae on the mutant appeared to feed randomly on the entire leaf, individuals consuming the Col–0 wild–type tended to ingest the leaf tissue between the midvein and the margin or edge (Scheme 3). Because the only difference between the two lines is their glucosinolate hydrolysis, it was automatic to suppose that such larval feeding behavior was influenced by the presence of glucosinolate hydrolysis products. But this supposition raised a question: Does the feeding pattern of *H. armigera* mean that the glucosinolates and their hydrolysis products are not evenly distributed in leaves? To address this question, mass spectrometry imaging was applied to examine the fine scale distribution of glucosinolates in *A. thaliana* leaves (see chapter 2.2).

Scheme 3. Feeding behavior of *Helicoverpa armigera* on *Arabidopsis thaliana* Col-0. 1st and 2nd instars tend to avoid feeding on the midvein or on the edge of 4–week–old rosette leaves. Picture represents the combined feeding activity of ten caterpillars over 5 hours. Photograph by Danny Keßler.

Mode of action of glucosinolates

Despite all the information compiled to date that supports the role of glucosinolate hydrolysis products as effective chemical defenses against many types of insect herbivores, their mode of action remains unknown. In the scope of plant–herbivore interactions the mode of action of a specific plant metabolite can be defined as the sequence of key events and processes starting with the interaction of the metabolite with an insect cell or biomolecule, proceeding through physiological and/or anatomical changes and resulting in deterrency or intoxication. As part of a project conceived to determine the mode of action of glucosinolates on insect herbivores, labeled glucosinolates are now being synthesized for use as tracers. Considering that the main glucosinolate produced by *A. thaliana* Col-0 is 4–methylsulfinylbutylglucosinolate (glucoraphanin), my efforts have centered on producing a labeled derivative of this compound. Because 4–methylsulfinylbutylglucosinolate bears an asymmetric sulfoxide, this compound has two epimers. For tracking the metabolism of any compound it is desirable to synthesize a molecule that resembles as accurately as possible the parental compound. However, it was found no method available for determining either the enantiomeric purity or the absolute configuration of the sulfoxide of 4–

methylsulfinylbutylglucosinolate. Therefore methods based on NMR spectroscopy were developed for achieving both objectives (see chapter 2.3). Using this information, a labelled 4–methylsulfinylbutylglucosinolate can now be produced matching the sterochemistry of the natural compound. Understanding the mode of action of any substance acting as chemical defense is important because it provides a mechanistic perspective of its toxicology and allows to test structure–activity relationships. In addition, if one knows what cell and molecular processes are affected by glucosinolates it might be easier to understand the structural diversity of this family of secondary compounds and to evaluate their ecological–evolutionary impact as regulators of plant–herbivore interactions.

References

[1] Barth C., Jander G. 2006. Arabidopsis Myrosinases TGG1 and TGG2 Have Redundant Function in Glucosinolate Breakdown and Insect Defense. *The Plant Journal*, 46(4): 549–562.

[2] Dearing M., Foley W., McLean S. 2005. The Influence of Plant Secondary Metabolites on the Nutritional Ecology of Herbivorous Terrestrial Vertebrates. *Annual Review in Ecology and Evolutionary Systematics*, 36: 169–189.

[3] Firempong S., Zalucki M. 1989. Host Plant Preferences of Populations of Helicoverpa-Armigera (Hubner) (Lepidoptera, Noctuidae) From Different Geographic Locations. *Australian Journal of Zoology*, 37(6): 665–673.

[4] Halkier B., Gershenzon J. 2006. Biology and Biochemistry of Glucosinolates. *Annual Review of Plant Biology*, 57: 303–333.

[5] Howe G., Jander G. 2008. Plant Immunity to Insect Herbivores. *Annual Review of Plant Biology*, 59: 41–66.

[6] Kjaer A. 1960. Naturally Derived *iso*Thiocyanates (Mustrad Oils) and their Parent Glucosides. *Fortschritte der Chemie Organischer Naturstoffe*, 18: 122–176.

[7] Lykkesfeldt J., Lindberg B. 1993. Synthesis of Benzylglucosinolate in *Tropaeolum majus* L. *Plant Physiology*, 102(2): 609–613.

[8] Richards O. 1940. The Biology of the Small White Butterfly (*Pieris rapae*), with Special Reference to the Factors Controlling its Abundance. *The Journal of Animal Ecology*, 9(2): 243–288.

[9] Wittstock U., Kliebenstein D., Lambrix V., Reichelt M., Gershenzon J. 2003. In: *Recent Advances in Phytochemistry*, 37: 101–125.

[10] Wittstock U., Agerbirk N., Stauber E., Olsen C., Hippler M., Mitchell-Olds T., Gershenzon J., Vogel H. 2004. Successful Herbivore Attack due to Metabolic Diversion of a Plant Chemical Defense. *PNAS*, 101(14): 4859–4864.

2. 1. Manuscript I

Chembiochem (2006)

Glycine Conjugates in a Lepidopteran Insect Herbivore–The Metabolism of Benzylglucosinolate in the Cabbage White Butterfly, *Pieris rapae*

Fredd Vergara, Aleš Svatoš, Bernd Schneider, Michael Reichelt,

Jonathan Gershenzon, and Ute Wittstock

Max–Planck–Institut für chemische Ökologie

Beutenberg Campus, Hans–Knöll–Str. 8, 07745 Jena

Abstract

Herbivores have developed a wide array of countermeasures to overcome plants' chemical defences. Larvae of the cabbage white butterfly, *Pieris rapae*, feed exclusively on plants of the Brassicales order, which are defended by the glucosinolate-myrosinase system. The defensive function of this system comes from toxic isothiocyanates that are formed when glucosinolates are hydrolyzed by myrosinases upon tissue damage. Here we show that *P. rapae* larvae convert benzylglucosinolate to phenylacetylglycine, which is released in their faeces. Feeding experiments with isotopic tracers suggest that phenylacetonitrile and phenylacetic acid are intermediates in this conversion. We also identified additional glycine and isoserine (2–hydroxyl–3–aminopropanoic acid) conjugates with benzoate and indole–3 carboxylate from *P. rapae* faeces extracts. This is the first description of such conjugates from lepidopteran insects.
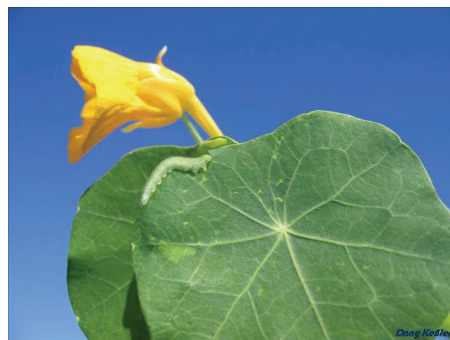
P. rapae larvae feeding on *Tropaeolum majus* leaves.

Photograph by Danny Keßler.

Introduction

Herbivore pressure has been recognized as a major driving force in the evolution of plants' chemical defences. In turn, plants' chemical defences are thought to be one of the major factors directing the evolution of phytophagous organisms[1]. Insect herbivores have developed a range of countermeasures against plants' chemical defences, including behavioural adaptations that allow insects to circumvent poisoning[2], as well as biochemical mechanisms such as insensitivity to toxins[3], sequestration of toxins in a physiologically safe manner[4], rapid excretion[5] or detoxification by phase I and phase II enzymes[6, 7]. Insect herbivores feeding on plants whose defences are activated by damage have also developed counteradaptations that interfere with the activation process. Two reactions that block the deployment of activated defences have recently been described for the diamond-back moth, *Plutella xylostella* (Lepidoptera: Plutellidae), and the cabbage white butterfly, *Pieris rapae* (Lepidoptera: Pieridae). Larvae of these insect herbivores feed exclusively on plants of the Brassicaceae and some related families, which employ the glucosinolate–myrosinase system as an activated chemical defence system[8, 9]. Glucosinolates, a group of nontoxic thioglycosides containing a (*Z*) –*N*–hydroximinosulfate ester group and a variable side chain (*e.g.*, compounds **1**, **2**, and **3**; Scheme 1A), are stored separately from their hydrolytic enzymes, the thioglucosidases, which are also known as myrosinases (EC 3.2.1.147) in the intact plant[10–12]. Upon tissue damage, for example by herbivory, glucosinolates and myrosinases come into contact, and the glucosinolates are hydrolyzed to their aglycones, which are unstable and rearrange into biologically active products (Scheme 1B)[13]. The most common type of hydrolysis products, the isothiocyanates, for example 4, have been shown to be toxic to a wide range of organisms, including insects[14–16]. *P. xylostella* and *P. rapae* overcome the glucosinolate-myrosinase defence system of their host plants by preventing the formation of the toxic isothiocyanates, by using two different biochemical mechanisms. Larvae of *P. xylostella* possess a highly active glucosinolate sulfatase (EC 3.1.6) in their gut that desulfates glucosinolates into desulfoglucosinolates that are no longer substrates for myrosinases[8]. *P. rapae* larvae express a gut protein designated, nitrile-specifier protein (NSP) that redirects the hydrolysis reaction towards the formation of nitriles instead of the toxic isothiocyanates (Scheme 1B)[19].
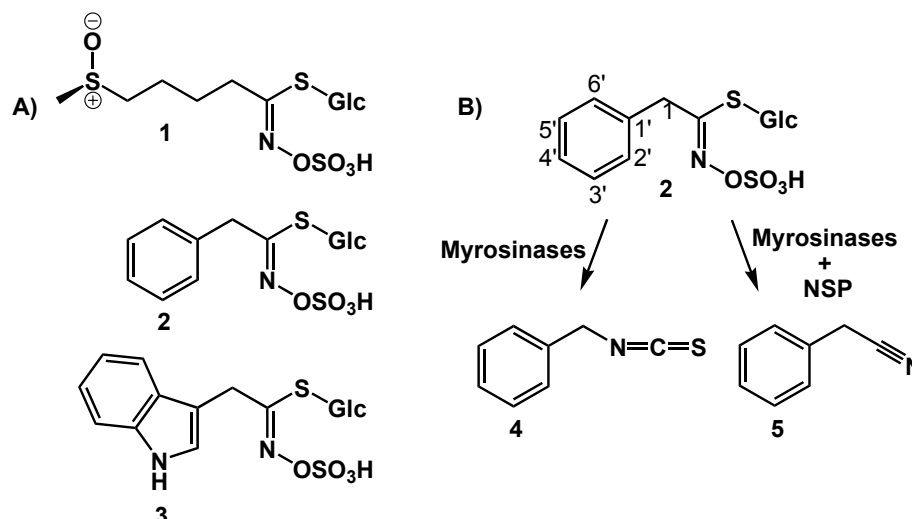
Scheme 1. **Chemical structure of glucosinolates and glucosinolate hydrolysis products generated by myrosinases and nitrile specifier protein (NSP).** A) Examples of glucosinolate structures with aliphatic (4–methylsulfinylbutylglucosinolate, **1**), benzenoid (benzylglucosinolate, **2**) and heterocyclic (indol–3–ylmethylglucosinolate, **3**) side chains. B) Hydrolysis of **2** by myrosinases and *P. rapae* NSP *in vitro*. Myrosinases catalyze the hydrolysis of the thioglucosidic bond of glucosinolates yielding glucose and an unstable aglucone. The aglucone rearranges spontaneously into the isothiocyanate (benzyl isothiocyanate, **4**). In the presence of NSP, the myrosinase–catalyzed hydrolysis is redirected towards the formation of the corresponding nitrile (phenylacetonitrile, **5**). Glc represents the β–D–glucose residue.

Nitriles derived from glucosinolates with aliphatic side chains, and from 4– hydroxybenzylglucosinolate have been shown to be excreted with the faeces[9]. NSP appears to be an enzyme that catalyses the conversion of the unstable aglycones generated by myrosinases into their corresponding nitriles[17]. Consonant with its ecological role to prevent isothiocyanate formation from diverse glucosinolates present in the larval food plant, NSP has a broad substrate specificity and accepts aglycones derived from glucosinolates with saturated and unsaturated alkyl sidechains, as well as benzylglucosinolate with its aromatic side chain[17]. Among the host plants of *P. rapae*, *Tropaeolum majus* (Tropaeolaceae) contains only one major

glucosinolate, the aromatic benzylglucosinolate (**2**), in its leaves[18, 19]. In preliminary studies of the metabolism of **2** in *P. rapae* larvae, we were unable to detect the corresponding nitrile, phenylacetonitrile (**5**) in larval faeces in quantities that were in accordance with the amounts of **2** that were ingested by the larvae (Wittstock, personal observation) even though **2** was efficiently converted to **5** by myrosinase in the presence of NSP *in vitro*. This raised the question of how **2** is actually metabolized by *P. rapae*, and whether NSP is involved in the metabolic pathway *in vivo*. Here, we present evidence that the major metabolite of benzylglucosinolate in *P. rapae* is phenylacetylglycine (**7**) and suggest a metabolic pathway for the formation of 7 based on feeding experiments with isotopic tracers.

Results

To test if benzylglucosinolate (**2**) or its metabolite(s) are excreted with the faeces or are retained in the larvae, we performed feeding experiments with radiolabelled benzylglucosinolate. *P. rapae* larvae were allowed to feed on leaves of *A. thaliana* that had taken up [1,1',2',3',4',5',6'–^{14}C7]benzylglucosinolate (^{14}C– labelled **2**, Scheme 1B). After consumption of the leaves, larvae and faeces were analyzed for radioactivity. In four independent experiments, 94–99% of the total radioactivity recovered from larvae and faeces was found in the faeces (representing 55–65% of the total radioactivity taken up by the leaves). Of the radioactivity in the faeces extracts, about 80% was detected in the aqueous extract and about 20% in the organic extract. HPLC analyses showed the presence of at least four radiolabelled compounds in the aqueous faeces extract, which were different from ^{14}C–labelled **2**, based on their retention times (Figure 1). The largest peak in the chromatogram represented about 70% of the total radioactivity in the HPLC sample. In *A. thaliana* leaves that had taken up ^{14}C–labelled **2**, but had been protected from larval feeding, the radiotracer remained intact throughout the experiment as demonstrated by HPLC (Figure 1). Thus, the radiolabelled compounds that were detected in the aqueous faeces extracts must be metabolites of ^{14}C–labelled **2** that were generated by the larvae.
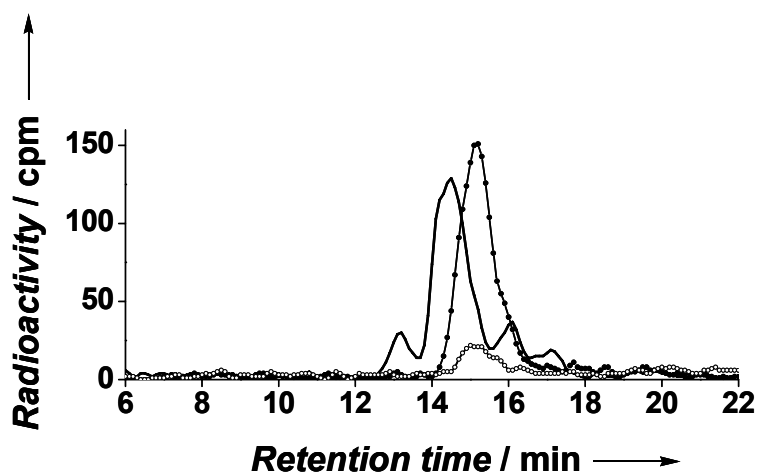
Figure 1. Metabolic fate of [^{14}C]benzylglucosinolate in larvae of *P. rapae*. Larvae were allowed to feed on detached rosette leaves of *A. thaliana* which had taken up [^{14}C]benzylglucosinolate. Their feces were collected and extracted with dichloromethane/water (1:1). The aqueous phase was analyzed by HPLC (bold line). As a control, *A. thaliana* leaves which had taken up [^{14}C]benzylglucosinolate and were left at room temperature for 12 h but were not fed on by *P. rapae*, were extracted with 80 % methanol after heat treatment to deactivate myrosinase and analyzed by HPLC (-•-). In addition, the [^{14}C]benzylglucosinolate tracer was analyzed directly by HPLC (-o-). Depicted are chromatograms recorded by a flow-through radioactivity detector.

To learn more about the chemical nature of the major metabolite of **2**, we performed similar feeding experiments using [1–^{13}C]benzylglucosinolate (^{13}C–labelled **2**, Scheme 1B). HPLC–MS analyses of the aqueous faeces extract performed in the positive fixed-product ion scan mode at *m/z* 91, showed the presence of at least three benzenoid compounds with different degrees of ^{13}C–labelling (Figure 2 A). The mass spectrum of the most strongly labelled compound had a molecular adduct ion ([M+H]$^{\oplus}$) of *m/z* 194, which is indicative of the presence of an odd number of nitrogen atoms in the molecule. Fixed precursor scan spectra showed consecutive losses of H$_2$O (*m/z* 176), CO (*m/z* 148), and CH$_2$=NH (*m/z* 119). To account for the presence of *m/z* 119 and to accommodate the benzylic group (*m/z* 91), it seemed likely that the benzylic moiety was directly bound to a carbonyl group (Scheme 2). The remainder of the molecule, which gave *m/z* 76, seemed likely to be a glycine residue given the sequence of losses from the molecular adduct ion. The compound was strongly labelled with an isotopic enrichment of 47% for ^{13}C (Figure

2A). A precursor ion scan of the *m/z* 195 isotopomer showed that the phenylacetyl and tropilium ions (*m/z* 120 and 92, respectively) were ^{13}C–enriched, but not that at *m/z* 76; this is consistent with the presence of ^{13}C atoms from the ^{13}C–labelled **2** being in the benzylic position.
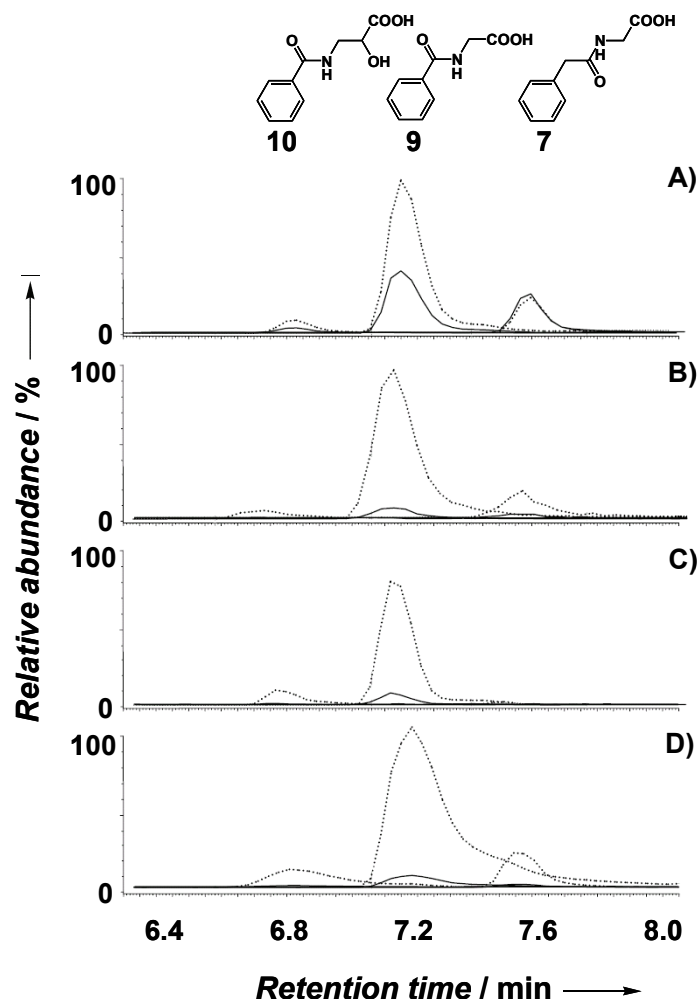

Figure 2. Specific isotopic enrichment of compounds detected in feces extracts of *P. rapae.* Larvae were allowed to feed on leaves of *A. thaliana* (Col–0) which had taken up [1–^{13}C]benzylglucosinolate (A), on *A. thaliana* 35S:CYP79A2 plants which accumulate benzylglucosinolate (B), on *A. thaliana* (Col–0) devoid of benzylglucosinolate (C), or on *T. majus* plants with high benzylglucosinolate content (D). Feces extracts prepared as described in the experimental section were analyzed by HPLC–MS using Multiple Reaction Monitoring (MRM) scanning mode. Dashed plots indicate ^{12}C and solid plots ^{13}C isotopomers, respectively. Parent compounds were *N*–benzoylisoserine (10),

hippuric acid (9), and phenylacetylglycine (7), listed in order of elution.

For further structure elucidation, the ^{13}C–labelled metabolites of **2** were isolated by semipreparative HPLC for NMR analysis. The ^{1}H, ^{13}C and 2D NMR spectra of the metabolite isolated from fraction F2, together with the mass spectrometric data suggested that the major metabolite of benzylglucosinolate that is produced by *P. rapae* larvae is phenylacetylglycine (2–(2–phenylacetamido)acetic acid, **7**, Scheme 2). The structure of this metabolite was confirmed by comparison of its MS and ^{1}H NMR spectra with those of an authentic standard of **7**, which was obtained commercially. The enhanced signal of the benzylic C–5 in the ^{13}C NMR spectrum, and the large satellites of 5–CH_2 in the corresponding ^{1}H NMR spectrum, which are due to [1]H–[13]C coupling ($^1J_{H-C}$=128 Hz), indicated specific ^{13}C enrichment in this methylene group.


7
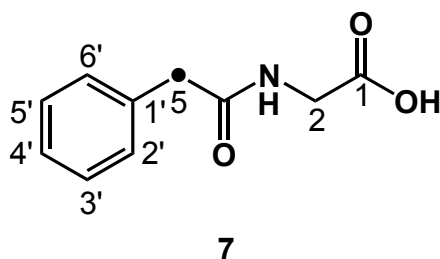
Scheme 2. Structure of the main metabolite of benzylglucosinolate in larvae of *P. rapae*. The main metabolite of [1–^{13}C]benzylglucosinolate, [5–^{13}C]phenylacetylglycine (**7**), was isolated from aqueous feces extracts obtained from larvae that were allowed to feed on detached rosette leaves of *A. thaliana* Col–0 which had taken up [1–^{13}C]benzylglucosinolate. ●=[13]C.

To prove that the formation of **7** from **2** is not due to the experimental conditions employed (*i.e.*, the use of leaves infiltrated with **2** rather than intact plants), we analyzed faeces extracts of larvae which had fed on *A. thaliana* 35S:CYP79A2 plants[20] containing **2**, and compared their composition with that of faeces extracts obtained after larvae had fed on wildtype plants devoid of **2** (Figure 2). Conjugate **7** was present in faeces extracts that were obtained after feeding on *A. thaliana* 35S:CYP79A2 plants (Figure 2B), but was not detected in faeces extracts from larvae feeding on wild-type plants lacking **2** (Figure 2C). We also evaluated the relevance of the formation of **7** under natural conditions by analyzing faeces produced by larvae

that were raised on *T. majus* plants that accumulate large amounts of 2 as their major glucosinolate. HPLC–MS chromatograms of the aqueous faeces extracts of *T. majus*–fed larvae showed the presence of large amounts of **7** (Figure 2D). Thus, the metabolism of **2** to **7** is not an artefact of the experimental design, but a major route of metabolism of **2** under natural conditions.

A possible route of formation of **7** is the conjugation of phenylacetic acid (**6**) with glycine (**8**; Scheme 3A). Compound **6** could be generated from phenylacetonitrile (**5**), a product of myrosinase–mediated hydrolysis of **2** in the presence of NSP. To test this hypothesis, we performed feeding experiments with putative precursors of **7** that were isotopically labelled. Water soluble tracers were fed to *P. rapae* larvae after they had been taken up by detached rosette leaves of *A. thaliana* Col–0, whereas lipophilic compounds were directly injected into *P. rapae* midguts through their mouths. Faeces extracts were then analyzed by HPLC–MS. When we fed ^{13}C–labelled **2**, the resulting conjugate **7** was labelled at position 5 (Scheme 3B); the same labelling pattern was obtained after feeding on the ^{13}C–labelled nitrile 5 and the ^{13}C–labelled acid **6** (Scheme 3B). These results are in agreement with the hypothesis that **2** is hydrolyzed to the corresponding nitrile **5**, which then undergoes hydrolysis to **6** (Scheme 3A). If this pathway were operating, the nitrogen atom of the conjugate **7** would originate from glycine (**8**) rather than from the glucosinolate. This was confirmed in feeding experiments with the ^{15}N–labelled nitrile **5** and [^{15}N]glycine (**8**). Feeding of [^{15}N]glycine (**8**) to leaves of *A. thaliana* 35S:CYP79A2 led to the incorporation of the labelled nitrogen atom into the conjugate **7** (32% ^{15}N incorporation) in larval faeces, while the nitrogen atom of the ^{15}N–labelled nitrile **5** was not incorporated in similar feeding experiments (Scheme 3B).
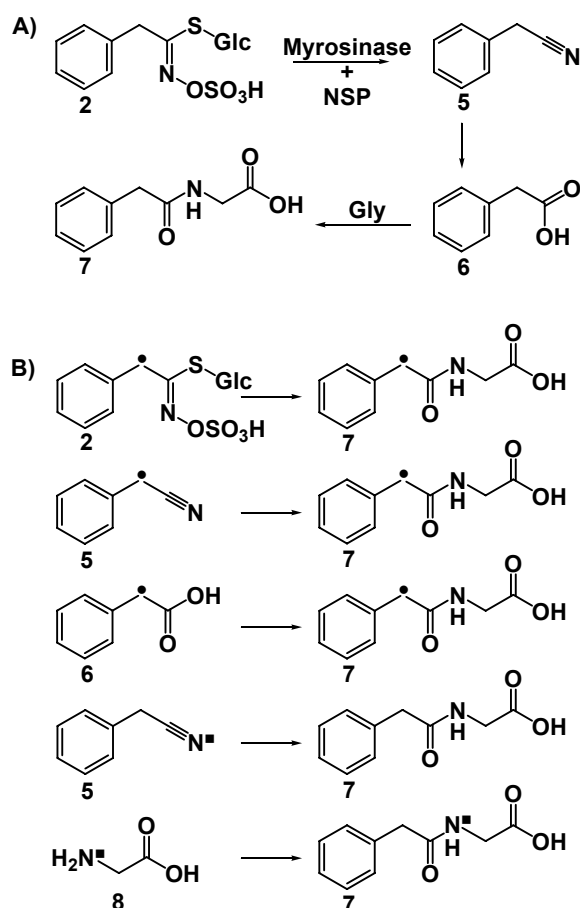
Scheme 3. Precursor and putative intermediates in the metabolic pathway from benzylglucosinolate to phenylacetylglycine. A) Possible reaction sequence leading from benzylglucosinolate (**2**) to phenylacetylglycine (**7**). B) Incorporation of putative precursors (left) into **7** (right) in feeding experiments with larvae of *P. rapae*. Larvae were either allowed to feed on *A. thaliana* leaves which had taken up isotopically labelled compounds (**2**, **6**, **8**) or were directly injected with the tracers (**5**). Feces were collected, and aqueous feces extracts were analyzed by HPLC–MS. The tracers used were [1–^{13}C]benzylglucosinolate (**2**), [2–^{13}C]phenylacetonitrile (**5**), [2–^{13}C]phenylacetic acid (**6**), [^{15}N]phenylacetonitrile (**5**), and [^{15}N]glycine (**8**). ●=^{13}C, ■=^{15}N.

Apart from the major metabolite phenylacetylglycine (**7**), we found two other ^{13}C–labelled metabolites in the aqueous faeces extract produced after feeding of [1–^{13}C] benzylglucosinolate (^{13}C–labelled **2**) to the larvae. These compounds displayed a lower isotopic enrichment than the main metabolite **7** (Figure 2), and were identified as amino acid *N*–conjugates of benzoic acid with either glycine (fraction F1, hippuric acid, **9**, *m/z* 180, [M+H]$^{⊕}$, 27% ^{13}C incorporation) or isoserine (fraction F3, *N*–

benzoylisoserine, **10**, *m/z* 210, [M+H]$^{\oplus}$, 24% ^{13}C incorporation; Scheme 4A). The ^{1}H NMR spectrum of compound **9** showed signals for a monosubstituted phenyl ring at δ=7.86, 7.54 and 7.47 and a methylene singlet at δ=4.08 (H–2). HMBC cross correlations through three bonds from H–2'/ H–6' (δ=7.86) to the carbonyl carbon atom at δ= 170.4, and from the methylene group to the same carbon suggested that this carbonyl must be located between the phenyl moiety and the methylene group. The extraordinary intensity of these cross-correlation peaks indicated that the carbonyl was enriched with ^{13}C. Because the MS fragmentation pattern of **9** gave evidence for a glycine residue, the structure was deduced to be *N*-benzoylglycine (hippuric acid) with the ^{13}C label at the benzoyl carbon.

The ^{1}H NMR spectrum of compound **10** displayed signals for a monosubstituted phenyl ring, and a three–spin system consisting of a hydroxymethine and two methylene protons. Together with the mass spectral information, these data were consistent with an *N*–benzoylisoserine structure **10**. Due to the very small amount of material available, the ^{13}C NMR spectrum did not show any of the natural abundance carbon signals. However, it exhibited a single enriched ^{13}C signal at δ=169.6 (C–5); this indicates that the label is on the benzoyl carbon. Compounds **9** and **10** are probably derived from metabolites of the glucosinolate **2** after the loss of a C1 unit from the glucosinolate side chain. Incorporation of label from [^{15}N]glycine (**8**) into the conjugate **9** in a feeding experiment in which *P. rapae* larvae ingested leaves of *A. thaliana* 35S:CYP79A2 plants infiltrated with [^{15}N]glycine (**8**) is in agreement with **9** being formed by conjugation with **8**.

In addition to the metabolites of the glucosinolate **2**, we identified two amino acid conjugates of indole–3–carboxylic acid in the aqueous faeces extracts of *P. rapae* (Scheme 4 B), *N*–(indole–3–carboxyl)glycine (**11**, *m/z* 219, [M+H]δ) and *N*–(indole–3–carboxyl)isoserine (**12**, *m/z* 249, [M+H]δ). The ^{1}H NMR spectra of both compounds displayed the characteristic fingerprint of an indole moiety: signals of an AMRX spin–system, including the downfield doublet of H–4' (**11**: δ=8.09; **12**: δ=8.08), and the additional singlet of H–3' (**11**: δ=7.97; 12: δ=7.91). The side-chain signals resembled those of compounds **9** and **10**, respectively. These data were supported by the mass spectra, which indicated compounds **11** and **12** as the indole analogues of the benzoic acid conjugates **9** and **10** (Scheme 4A). Accordingly, compounds **11**

and **12** might be biotransformation products of indole glucosinolates, for example, of indol–3–ylmethylglucosinolate (**3**, Scheme 1), after loss of a C1 unit. Another possibility is that they originate from other compounds bearing an indole moiety. Both compounds were present in all faeces extracts analyzed, including those from larvae reared on *T. majus* plants. In feeding experiments with [^{15}N]glycine (**8**), the labelled nitrogen atom was incorporated into **11** (36% ^{15}N incorporation), but not into **12**.
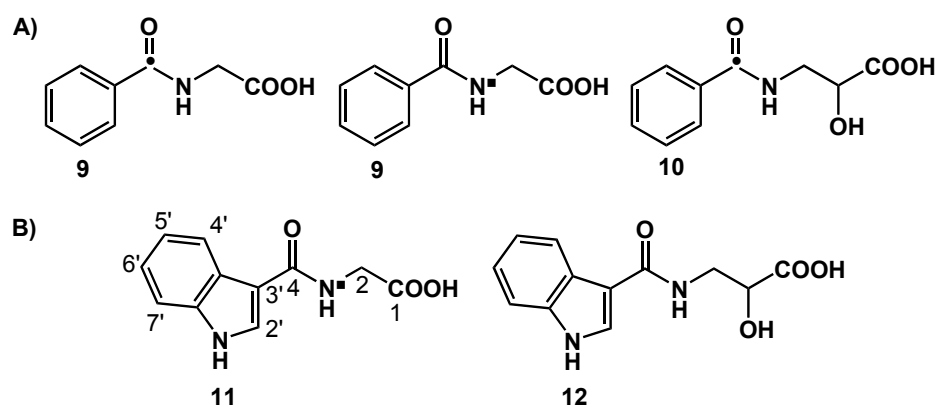
Scheme 4. Additional amino acid conjugates identified in feces of *P. rapae*. A) Labelling pattern of metabolites of benzylglucosinolate identified in feces extracts of larvae which had fed on *A. thaliana* (Col–0) leaves which had taken up [1–^{13}C]benzylglucosinolate or on *A. thaliana* (35S:CYP79A2) leaves which had taken up [^{15}N]glycine. B) Indolic amino acid conjugates identified in *P. rapae* feces extracts. **9**, hippuric acid, **10**, *N*–benzoylisoserine, **11**, *N*–(indole–3–carboxyl)glycine, **12**, *N*–(indole–3–carboxyl)isoserine. ●=^{13}C, ■=^{15}N.

Discussion

Insect herbivores can circumvent an activated plant defence system, such as the glucosinolate–myrosinase system, in several different ways. On the one hand, they can prevent the release of toxic hydrolysis products by metabolising glucosinolates before myrosinases can act on them, by inhibiting the myrosinases, or by changing the outcome of the myrosinasecatalysed reaction. On the other hand, insects can detoxify hydrolysis products once they are formed. Here we show that more than one of these mechanisms is involved in the detoxification of benzylglucosinolate (**2**) in larvae of *P. rapae*. First, larval NSP diverts glucosinolate hydrolysis to phenylacetonitrile (**5**) instead of the corresponding isothiocyanate. Then, **5** is metabolized by oxidation to phenylacetic acid (**6**), a phase I detoxification reaction, and by conjugation with glycine (**8**), a phase II detoxification reaction. The resulting phenylacetylglycine (**7**, Scheme 2) is excreted with the faeces (Figure 1, Scheme 3A). This reaction sequence was deduced from feeding experiments with isotopically labelled precursors in which the label from ^{13}C–labelled **2**, ^{13}C–labelled **5**, ^{13}C–labelled **6**, and ^{15}N–labelled **8** was incorporated into the conjugate **7** while there was no incorporation of the label from ^{15}N–labelled **5** (Scheme 3B).

The oxidation of a nitrile to the corresponding carboxylic acid, and the conjugation of the acid with glycine have not yet been demonstrated in insects, and it could be that enzymes from the ingested plant material or gut microorganisms are involved. So far nitrilases (EC 3.5.5.1) that hydrolyze nitriles to their corresponding acids have only been characterised from plants and microorganisms[21–23]. Alternatively, a nitrile hydratase (EC 4.2.1.84) could catalyse the formation of an amide, which would subsequently be hydrolyzed to the acid **6** by an amidase (EC 3.5.1.4). Nitrile hydratases as well as amidases are frequently found in microorganisms and have also been identified in plants[24–27]. Conjugation with glycine is a common route of metabolism for small carboxylic acids in mammals that requires activation of the acid by an acyl–CoA–synthetase (EC 2.3.1) prior to transfer of the acyl residue to glycine, which is catalysed by an *N*–acyltransferase (EC 2.3.1.13)[28]. However, to our knowledge, glycine conjugates have not previously been reported in lepidopteran insects.

Apart from the major metabolite phenylacetylglycine (**7**), we also identified benzoic acid conjugates with glycine and isoserine as metabolites of benzylglucosinolate (2) in *P. rapae* by HPLC–MS (Scheme 4). Whether these compounds also correspond to the minor peaks detected by HPLC with radioactivity detection, however, remains uncertain. Formation of the benzoyl moiety from **2** is likely to occur via phenylacetonitrile (**5**) and phenylacetic acid (6) intermediates, with the subsequent loss of a C1 unit. However, the conversion of phenylacetic acid to benzoic acid has never been demonstrated in biological systems. ^{13}C–labelled benzoic acid conjugates with glycine (**9**, 27% ^{13}C incorporation) and isoserine (**10**, 24% ^{13}C incorporation) were found in faeces extracts after *P. rapae* larvae had fed on leaves containing ^{13}C–labelled **2**, but their unlabelled counterparts were also detected in faeces extracts of larvae which had fed on leaves of *A. thaliana* Col-0, which is devoid of **2** (Figure 2). However, we could not find the conjugate **7** in the larval faeces extracts after the larvae had fed on *A. thaliana* that was devoid of **2**; this is consistent with **7** being a major metabolite of **2** (Figure 2). These results also show that conjugation with glycine and the unusual nonprotein amino acid isoserine could be a common pathway for metabolism of endogenous or exogenous compounds in *P. rapae*, a conclusion that is also supported by the identification of glycine and isoserine conjugates of indole–3–carboxylic acid in the faeces extracts from all feeding experiments (Scheme 4). The degradation of indole glucosinolates to indole–3–carboxylic acid derivatives has been suggested to occur in plants upon infection with an oomycete[29]. Whether or not the conjugates identified in our study are derived from indole glucosinolates still needs to be investigated. However, they were also detected in faeces extracts of larvae that had fed on *T. majus* leaves, which to our knowledge do not contain indole glucosinolates18. This suggests that they are derived from other indolic precursors.

The nitriles derived from glucosinolate hydrolysis are generally considered to be less toxic than their isothiocyanate counterparts[14]. In previous work, we found that nitriles arising from diversion of the hydrolysis of aliphatic glucosinolates by *P. rapae* NSP were excreted with the faeces without apparent ill effects[9]. Nevertheless, certain nitriles are further metabolized by different pathways. 4–hydroxyphenylacetonitrile, derived from 4-hydroxybenzylglucosinolate, is converted into its sulfate ester prior to excretion[9, 30], and here we have demonstrated that the oxidation of the nitrile **5**, derived from benzylglucosinolate, leads to the acid **6**, and

that the conjugation of **6** leads to **7**. The differential metabolism of nitriles might be a consequence of differences in their toxic potential.

The formation of amino acid conjugates in insects has only rarely been studied with respect to detoxification processes[28, 31, 32]. However, fatty acid–amino acid conjugates are abundant components of the gut content of lepidopteran larvae and other insects, and have been proposed to act as surfactants during digestion[33]. Conjugates of fatty acids with glutamine or glutamic acid, which is present in oral secretions of lepidopteran larvae, have been demonstrated to be elicitors of plant defence responses upon herbivore attack[34, 35]. Depending on the insect species, these conjugates are synthesised by gut microorganisms or membrane-associated enzyme(s) of alimentary tissues[36, 37]. Future work will investigate the enzymatic machinery engaged in the formation of glycine conjugates to shed light on the evolutionary relationships between the conjugating enzymes involved in biosynthetic pathways, and detoxification processes.

In previous investigations, *P. rapae* was shown to metabolize aliphatic glucosinolates into nitriles *in vivo*[9]. Here, we demonstrate that benzylglucosinolate, a compound that is highly abundant in *T. majus*, which is one of the common host plants of *P. rapae* is converted principally to a glycine conjugate. Compared to the detoxification mechanism employed by the diamond-back moth, *Plutella xylostella*, which produces a single enzyme to efficiently convert all glucosinolates to the nontoxic desulfoglucosinolates[8], the machinery employed by *P. rapae* larvae to overcome the chemical defences of their host plants is apparently much more complex. Future investigations will try to determine if the additional costs that are likely associated with the multifaceted metabolism of glucosinolates in *P. rapae* are compensated for by their ability to use a wider range of host plants.

Experimental Section

Plant culture: *A. thaliana* (Brassicaceae) was grown in a controlled environment chamber at 21°C and 55% humidity with a photoperiod of 14 h, at a light intensity of 230 µmol m^{-2} s^{-1}. Two different types of *A. thaliana* plants were used: wild-type plants of the ecotype Columbia (Col–0) and the transgenic 35S:CYP79A2 plants, which accumulate high amounts of benzylglucosinolate[20]. *T. majus* was grown in a greenhouse at 21°C and 55% humidity. Supplemental illumination was provided by Philips Sun–T Agro 400 and 600 W sodium lights (Eindhoven, NL), which produced a light intensity of 185 µmol m^{-2} s^{-1} for 14 h per day.

Insect culture: A continuous culture of *P. rapae* was maintained on Brussels sprouts plants (*Brassica oleracea* convar. fruticosa var. gemmifera cv. Rosella) in a controlled environment chamber at 22°C and 70% humidity with a photoperiod of 16 h. The culture originated from wild individuals collected by I. Mewis (Humboldt University, Berlin, Germany) in summer 2004. In parallel, a culture of *P. rapae* was maintained on *T. majus* after larvae were hatched on these plants.

Chemicals: The benzylglucosinolate (**2**) that was used as a reference was isolated from *Lepidium sativum* seeds as described previously[38]. Phenylacetylglycine (**7**) was purchased from Bachem (Bubendorf, Switzerland).

Isotopically labelled chemicals: *L*–[U–^{14}C]phenylalanine (17.4 Gbq mmol^{-1}, 1.85 MBq mL^{-1}) was purchased from GE Healthcare (Buckinghamshire, UK); *L*–[3–^{13}C]phenylalanine (99 atom% ^{13}C) was purchased from Sigma–Aldrich (Milwaukee, USA). To produce [1,1',2',3',4',5',6'–^{14}C7]benzylglucosinolate (^{14}C–labelled **2**, 225 MBq mmol^{-1}, 24 kBq mL^{-1}) and [1–^{13}C]benzylglucosinolate (^{13}C–labelled **2**, 40 atom% ^{13}C), we used a solution composed of [U–^{14}C]phenylalanine (500 mL) or [3–^{13}C]phenylalanine (500 mL, 100 mg mL^{-1}) and Murashige & Skoog (MS) medium (500 mL) divided into ten wells of a microtiter plate. Detached rosette leaves of 6–week–old *A. thaliana* 35S:CYP79A2 were inserted into the wells (2–5 leaves per well). When most of the liquid had been taken up by the leaves, MS medium (50 mL) was added to each well. After 12 h incubation, **2** was isolated[38] and converted into its protonated form[39]. In the purified preparation obtained after feeding of [U–^{14}C]phenylalanine, ^{14}C–labelled **2** accounted for 97% of the radioactivity present, as shown by HPLC analysis (system 1, detectors 1 and 2). In the experiment with [3–

[13C]phenylalanine, [13C]–labelled **2** was further purified by semipreparative HPLC (system 3, detector 1), which afforded a purity of more than 95% as estimated by HPLC. [2–[13C]]Phenylacetonitrile ([13C]–labelled **5**, 99 atom% 13C) was purchased from Sigma–Aldrich (Milwaukee, USA). [2–[13C]]Phenylacetic acid ([13C]–labelled **6**) was synthesised by hydrolysis of [13C]–labelled **5** with 15% H_2O_2 in 1N NaOH at room temperature, and the structure was confirmed by [1H] NMR spectroscopy. [[15N]]–Potassium cyanide (98 atom% [15N]) was purchased from Sigma–Aldrich (Milwaukee, USA). [[15N]]Phenylacetonitrile ([15N]–labelled **5**) was synthesised as previously described[40], and its identity was confirmed by HPLC–MS, and by [1H] and [15N] NMR spectroscopy. [[15N]]Glycine ([15N]–labelled **8**, 98 atom% [15N]) was purchased from Isotech (Miamisburg, USA).

HPLC and MS analysis: HPLC was performed on an HP1100 series instrument (Agilent Technologies, Waldbronn, Germany). Chromatographic conditions were as follows. System 1: The instrument was equipped with a Supelcosil LC–18DB column (250N2.1 mm, 5 mm particle size; Supelco, Taufkirchen, Germany). Elution was accomplished with a gradient of 0.1% (v/v) formic acid (FA, solvent A) and acetonitrile/FA (99.9:0.1 (v/v), solvent B) at a flow rate of 0.25 mLmin[-1] at 25°C as follows: 1.5–45% (v/v) B (15 min), 45–100% (v/v) B (1 min), 100% B (1 min), 100–1.5% (v/v) B (6 s), 1.5% (v/v) B (9.54 min). System 2: Same solvents and flow rate as system 1, but 1.5–45% (v/v) B (5 min), 45–100% (v/v) B (11 min), 100% B (5 min). System 3: The instrument was equipped with a Hypersil 5 ODS column (250N10 mm; Chromapack, Darmstadt, Germany). Elution was accomplished with a gradient of 0.1% (v/v) FA (solvent A) and acetonitrile/FA (99.9:0.1 (v/v), solvent B) at a flow rate of 4.0 mLmin[-1] at 25°C as follows: 1.5–33.4% (v/v) B (11 min), 33.4–100% (v/v) B (6 s), 100% B (1 min 24 s), 100–1.5% (v/v) B (6 s), 1.5% (v/v) B (9.54 min).

The instrument was connected with different detectors. Detector 1: UV detector (210 nm). Detector 2: Flow-through radioactivity detector (Radiomatic 500 TR, Packard, Dreieich, Germany) containing an 0.5 mL liquid fluid cell operated with Ultima Flow scintillation cocktail (Packard, Groningen, The Netherlands) used in a ratio of 4:1(v/v) to column eluent. Detector 3: Micromass Quattro II tandem quadrupole mass spectrometer (Micromass, Manchester, UK) equipped with an electrospray ionization (ESI) source. The capillary and cone voltages in ESI mode were 3.3 kV and 18 V, respectively. Nitrogen for nebulization was applied at 15 L h^{-1},

drying gas was applied at 250 L h^{-1} and 250°C. Source and capillary were heated at 80 and 150°C, respectively. The mass spectrometer was operated in conventional scanning mode using the first quadrupole. Negative–ion and positive–ion full–scan mass spectra were recorded from m/z 90–450 (scanning time: 1.5 s). Fixed precursor ion (MS/MS) spectra (daughter–ion scan) and fixed product spectra (parention scan) were recorded by standard methods[29]. Argon was used for collision–induced dissociations (CID) at 1.5 x 10^{-3} mbar and the collision energy was varied from 12–50 eV for fragmentation. For multiple reaction monitoring (MRM), the precursor ions were selected in the first quadrupole, fragmented in the collision cell, and the characteristic product ions were selected in the second quadrupole. The ion pairs used to detect the incorporation of native and ^{13}C–labelled **2** into metabolites were: unlabelled/^{13}C–labelled **7**: 194–76/195–76, **9**: 180–105/181–106, and **10**: 210–105/211–106. Isolated fractions were dissolved in methanol and were injected (ca. 5–10 mL) into the mobile phase (acetonitrile/water 1:1 (v/v), flow rate: 50 mL min^{-1}) using a Rheodyne valve. The percentage of isotopic incorporation I was calculated according to the equation:

$$I = \left(\frac{B_L}{A_L + B_L} - \frac{B_N}{A_N + B_N} \right) \times 100\%$$

in which A_L and A_N represent the spectral intensity of ^{12}C or ^{14}N peaks for labelled and native precursors, respectively; B_L and B_N represent the intensity of the corresponding ^{13}C or ^{15}N peaks for labelled and native precursors. Spectra measured for faeces extracts from larvae which had fed on *T. majus* were used to obtain spectral intensities of native precursors.

NMR spectroscopy: NMR spectra were measured on a Bruker AV500 NMR spectrometer (Bruker Biospin, Rheinstetten, Germany) equipped with a CryoPlatformTM. ^{1}H NMR, ^{13}C NMR, ^{1}H,^{1}H COSY, ^{1}H,^{1}H lrCOSY, HMBC and HSQC spectra were recorded by using a 5 mm TXI CryoProbe. Operating frequencies were 500.13 and 125.75 MHz for acquisition of ^{1}H and ^{13}C spectra, respectively. [d_4]MeOH was used as a solvent. Chemical shifts are reported relative to Me$_4$Si as internal standard.

Feeding experiments with tracers: In the experiments with labelled glucosinolates, detached rosette leaves of 4–5–week–old *A. thaliana* Col–0 plants were allowed to take up a mixture of ^{14}C–labelled **2** (50 mL) or ^{13}C–labelled **2** (50 mL) and MS medium (50 mL) in a 180 mL well of a microtiterplate (two leaves per well, ten wells in total). When they had taken up the liquid (in a typical experiment about 95% of the total radioactivity used), the leaves were either used for feeding experiments with insect larvae, or were kept protected from insect feeding and analyzed for intact, labelled glucosinolate after 12 h.

In the insect feeding experiments, the leaves were moved to a second microtiterplate. In this plate the wells had been filled with MS medium (50 mL), and the plate had been covered with a plastic foil with openings to insert the petioles. Larvae of *P. rapae* (typically 25 fourth–fifth instar larvae per 20 leaves), which were starved for 10 h before the experiment were then allowed to feed on the leaves. Their faeces were collected over a period of 12 h in 30 min intervals into sealed glass vials and stored at –20°C. Afterwards, larvae, faeces and the remains of leaves that were not consumed by the larvae were ground and extracted with dichloromethane (1 mL) and water (1 mL). After centrifugation (2000*g*, 5 min), the phases were separated. The extraction was repeated once, and the corresponding phases were combined. Leaves that had been protected from herbivory were dried at 90°C for 1 h to deactivate myrosinases, and were then extracted with 80% methanol. Insect feeding experiments with ^{13}C–labelled **6** and ^{15}N–labelled **8** were done as described above, but with ten leaves and five larvae per experiment. For feeding with ^{15}N–labelled **8**, *A. thaliana* 35S: CYP79A2 plants were used instead of Col–0 plants. Faeces were collected after 16 h and extracted as described above. ^{13}C–labelled **5** (1 mL) and ^{15}N-labelled **5** (1 mL) were injected directly into the midgut of five larvae through their mouth opening by using a microsyringe with a rounded tip needle. Afterwards, larvae were allowed to feed on *A. thaliana* Col–0. Faeces produced during the following 16 h were collected and extracted as described above. In the experiments with ^{13}C– and ^{15}N–labelled compounds, the aqueous faeces extracts were analyzed by HPLC–MS (system 2, detectors 1 and 3).

Feeding experiment with intact plants: *P. rapae* larvae reared on *T. majus* were allowed to feed *ad libitum* on these plants for two weeks. Faeces were collected, stored at –20°C and extracted with equal volumes of dichloromethane and

water as described above. The aqueous phase was analyzed by HPLC (system 2, detectors 1 and 3).

Analysis of extracts containing radiolabelled compounds: Radioactivity present in the extracts was measured on a Tri–carb 2300TR liquid scintillation analyzer (Packard, Dreieich, Germany) by using either Lumasafe or Lipoluma Plus liquid scintillation cocktails (LUMAC* LSC B.U., Groningen, The Netherlands). In the experiments with ^{14}C–labelled **2**, the aqueous faeces extract and the methanolic leaf extract were further analyzed by HPLC (system 1, detectors 1 and 2).

Isolation of benzylglucosinolate metabolites from faeces extract: The aqueous faeces extract (2 mL) that was obtained in the insect feeding experiment with ^{13}C–labelled **2** was concentrated to a final volume of 500 mL under a nitrogen stream at 50°C. The sample was passed over a phenyl–modified silica solid–phase extraction cartridge (Macherey–Nagel, DPren, Germany). After conditioning the cartridge with methanol (3 mL) and water (3 mL), the sample was loaded and eluted with methanol (4 mL). The eluate was concentrated to a final volume of approximately 500 mL under a nitrogen stream at 50°C. Aliquots of 100 mL were separated by semipreparative HPLC (system 3, detector 1). An SF–2120 fraction collector (Advantec, Japan) was used to collect fractions eluting at 10:45–11:10 min (F1), 11:12–11:24 min (F2) and 11:30–12:00 min (F3). The corresponding fractions that were obtained in different runs were pooled and dried under a nitrogen stream. Aliquots were analyzed by HPLC (system 1, detector 1) and HPLC–MS (system 2, detector 3). Samples were then dissolved in deuterated methanol for NMR analysis.

Analytical data for isolated metabolites

Phenylacetylglycine (**7**): ^{1}H NMR ([d_4]MeOH): δ=7.31 (m, 2H; H–2'/6'), 7.29 (m, 2H; H–3'/5'), 7.22 (m, 1H; H–4'), 3.88 (s, 2H; H–2), 3.57 ppm (s of H–5 attached to ^{12}C, and δ of H–5 attached to 13C, JH5–C5=128 Hz, 2H); ^{13}C NMR ([d_4]MeOH): δ=174.5 (C–4), 173.3 (C–1), 136.8 (C–1'), 130.2 (C–2'/5'), 129.6 (C–3'/5'), 127.9 (C–4'), 43.6 (C–5), 42.1 ppm (C–2); ESI–MS (8 eV) m/z (rel. intens.): 194 (90) [M+H]$^{\oplus}$, 176 (8) [M+H-H$_2$O]$^{\oplus}$, 148 (5) [M+H-HCO$_2$H]$^{\oplus}$, 119 (8), 91 (19), 76 (100); [5–^{13}C]**7**: ESI–MS (8 eV) m/z (rel. intens.): 195 (90) [M+H]$^{\oplus}$, 177 (8) [M+H-H$_2$O]$^{\oplus}$, 149 (5) [M+H-HCO$_2$H]$^{\oplus}$, 120 (8), 92 (19), 76 (100).

2– (Benzamido)acetic acid (hippuric acid; **9**): ^{1}H NMR ([d_4]MeOH): δ=7.86 (d, J=8.1 Hz, 2H; H–2'/6'), 7.54 (t, J=7.3 Hz, 1H; H–4'), 7.47 (dd, J=7.3 Hz, 8.1 Hz, 2H; H–3'/5'), 4.08 ppm (s, 2H; H–2); ^{13}C NMR ([d_4]MeOH): δ=173.3 (C–1), 170.4 (^{13}C–enriched, C–4), 135.1 (C–1'), 132.8 (C–4'), 129.5 (C–3'/5'), 128.4 (C–2'/6'), 42.4 ppm (Cv2); ESI–MS (8 eV) m/z (rel. intens.): 180 ([M+H]$^{\oplus}$, 53), 162 ([M+H-H$_2$O]$^{\oplus}$, 5), 134 ([M+H-HCO$_2$H]$^{\oplus}$, 105 (100); (25 eV): 105 (100), 77 (25). [4-^{13}C]9: ESIMS (8 eV) m/z (rel. intens.): 181 ([M+H]$^{\oplus}$, 53), 163 ([M+H-H$_2$O]$^{\oplus}$, 5), 135 ([M+H-HCO2H]$^{\oplus}$, 106 (100); (25 eV): 106 (100), 77 (25).

3–(Benzamido)–2–hydroxypropanoic acid (N–benzoyl–isoserine; **10**): ^{1}H NMR ([d_4]MeOH): δ=7.90 (d, J=8.1 Hz, 2H; H–2'/6'), 7.54 (t, J=7.3 Hz, 1H; H–4'), 7.47 (dd, J=7.3, 8.1 Hz, 2H; H–3'/5'), 4.52 (dd, J=5.0, 6.1 Hz, 1H; H–2), 3.57 (dd, J=5.0, 11.1 Hz, 1H; H–3a), 3.50 ppm (dd, J=6.1, 11.1 Hz, ^{1}H; H–3b); ^{13}C NMR ([d_4]MeOH): d=169.6 ppm (^{13}C enriched, C-5); ESI–MS (8 eV) m/z (rel. intens.): 210 (100) [M+H]$^{\oplus}$, 192 (21) [M+H-H$_2$O]$^{\oplus}$, 164 (9) [M+H-HCO$_2$H]$^{\oplus}$, 105 (51), 88 (16), 60 (9); [5–^{13}C]10: ESI–MS (8 eV) m/z (rel. intens.): 211 (100) [M+H]$^{\oplus}$, 193 (21) [M+H-H$_2$O]$^{\oplus}$, 165 (9) [M+H-HCO$_2$H]$^{\oplus}$, 106 (51), 88 (16), 60 (9).

2–(1H–indolyl–3–carboxyamido)acetic acid (N–(indole–3–carboxyl)glycine; **11**): ^{1}H NMR ([d_4]MeOH): δ=8.09 (d, J=8.0 Hz, 1H; H-4'), 7.91 (s, 1H; H–2'), 7.43 (d, J=8.0 Hz, 1H; H–7'), 7.19 (dd, J=8.0, 8.0 Hz, 1H; H–6'), 7.16 (dd, J=8.0, 8.0 Hz, 1H; H–5'), 4.11 ppm (s, 2H; H–2); ESI–MS (8 eV) m/z (rel. intens.): 219 (0.3) [M+H]$^{\oplus}$, 144 (100), 116 (7).

3–(1H–indolyl–3–carboxyamido)–2–hydroxypropanoic acid (*N*–(indole–3–carboxyl)isoserine; **12**): ^{1}H NMR ([d_4]MeOH): δ=8.08 (d, *J*=8.0 Hz, 1H; H–4'), 7.97 (s, 1H; H–2'), 7.44 (d, *J*=8.0 Hz, 1H; H–7'), 7.19 (dd, *J*=8.0, 8.0 Hz, 1H; H–6'), 7.17 (dd, *J*=8.0, 8.0 Hz, 1H; H–5'), 4.67 (dd, *J*=5.0, 6.1 Hz, 1H; H–2), 4.03 (dd, *J*=6.1, 11.1 Hz, 1H; H–3a), 3.97 ppm (dd, *J*=5.0, 11.1 Hz, 1H; H–3b); ESI–MS (8 eV) *m/z* (rel. intens.): 249 (31) [M+H]$^\oplus$, 144 (100).

Acknowledgements

References

[1] P. R. Ehrlich, P. H. Raven, Evolution 1964, 18, 586–608.

[2] D. E. Dussourd, T. Eisner, Science 1987, 237, 898–901.

[3] F. Holzinger, C. Frick, M. Wink, FEBS Lett. 1992, 314, 477–480.

[4] C. Naumann, T. Hartmann, D. Ober, Proc. Natl. Acad. Sci. USA 2002, 99, 6085–6090.

[5] L. S. Self, F. E. Guthrie, E. Hodgson, Nature 1964, 204, 300–301.

[6] G. W. Ivie, D. L. Bull, R. C. Beier, N. W. Pryor, E. H. Oertli, Science 1983, 221, 374–376.

[7] L. B. Brattsten in Herbivores: Their Interaction with Secondary Plant Metabolites, Vol. 2, (Eds.: G. A. Rosenthal, M. R. Berenbaum), Academic Press, San Diego, 1992, pp. 175–242.

[8] A. Ratzka, H. Vogel, D. J. Kliebenstein, T. Mitchell–Olds, J. Kroymann, Proc. Natl. Acad. Sci. USA 2002, 99, 11223–11 228.

[9] U. Wittstock, N. Agerbirk, E. J. Stauber, C. E. Olsen, M. Hippler, T. Mitchell- Olds, J. Gershenzon, H. Vogel, Proc. Natl. Acad. Sci. USA 2004, 101, 4859–4864.

[10] J. W. Fahey, A. T. Zalcmann, P. Talalay, Phytochemistry 2001, 56, 5–51.

[11] C. D. Grubb, S. Abel, Trends Plant Sci. 2006, 11, 89–100.

[12] L. Rask, E. Andreasson, B. Ekbom, S. Eriksson, B. Pontoppidan, J. Meijer, Plant Mol. Biol. 2000, 42, 93–113.

[13] F. S. Chew in Biologically Active Natural Products (Ed.: H. G. Cutler), American Chemical Society, Washington DC, 1988, pp. 155–181.

[14] U. Wittstock, D. J. Kliebenstein, V. Lambrix, M. Reichelt, J. Gershenzon in Integrative Phytochemistry: From Ethnobotany to Molecular Ecology, Vol. 37, (Ed.: J. T. Romeo) Elsevier, Amsterdam, 2003, pp. 101–125.

[15] A. A. Agrawal, N. S. Kurashige, J. Chem. Ecol. 2003, 29, 1403–1415.

[16] Q. Li, S. D. Eigenbrode, G. R. Stringam, M. R. Thiagarajah, J. Chem. Ecol. 2000, 26, 2401–2419.

17 M. Burow, J. Markert, J. Gershenzon, U. Wittstock, FEBS J. 2006, 273, 2432–2446.

18 R. N. Bennett, G. Kiddle, A. J. Hick, G. W. Dawson, R. M. Wallsgrove, Plant Cell Environ. 1996, 19, 801–812.

19 J. A. A. Renwick, K. Lopez, Entomol. Exp. Appl. 1999, 91, 51–58.

20 U. Wittstock, B. A. Halkier, J. Biol. Chem. 2000, 275, 14659–14666.

21 S. Vorwerk, S. Biernacki, H. Hillebrand, I. Janzik, A. MPller, E. W. Weiler, M. Piotrowski, Planta 2001, 212, 508–516.

22 H. C. Pace, C. Brenner, Genome Biol. 2001, 2, reviews 0001.1–0001.9.

23 C. O'Reilly, P. D. Turner, J. Appl. Microbiol. 2003, 95, 1161–1174.

24 H. Yamada, S. Shimizu, M. Kobayashi, Chem. Rec. 2001, 1, 152–161.

25 M. Kobayashi, T. Suzuki, T. Fujita, M. Masuda, S. Shimizu, Proc. Natl. Acad. Sci. USA 1995, 92, 714–718.

26 M. Piotrowski, S. Schçnfelder, E. W. Weiler, J. Biol. Chem. 2001, 276, 2616–2621.

27 S. Pollmann, D. Neu, E. W. Weiler, Phytochemistry 2003, 62, 293–300.

28 K. R. Huckle, P. Millburn, Prog. Pestic. Biochem. 1982, 2, 127–169.

29 P. Bednarek, B. Schneider, A. Svatosˇ, N. J. Oldham, K. Hahlbrock, Plant Physiol. 2005, 138, 1058–1070.

30 N. Agerbirk, C. MPller, C. E. Olsen, F. S. Chew, Biochem. Syst. Ecol. 2006, 34, 189–198.

31 L. Friedler, J. N. Smith, Biochem. J. 1954, 57, 396–400.

32 T. W. Jordan, C. K. Chang, J. N. Smith, Insect Biochem. 1980, 10, 265–271.

33 K.-G. Collatz, T. Mommsen, J. Comp. Physiol. 1974, 94, 339–352.

34 H. T. Alborn, T. C. J. Turlings, T. H. Jones, G. Stenhagen, J. H. Loughrin, J. H. Tumlinson, Science 1997, 276, 945–949.

35 R. Halitschke, U. Schittko, G. Pohnert, W. Boland, I. T. Baldwin, Plant Physiol. 2001, 125, 711–717.

36 D. Spiteller, K. Dettner, W. Boland, Biol. Chem. 2000, 381, 755–762.

37 C. G. Lait, H. T. Alborn, P. E. A. Teal, J. H. Tumlinson, Proc. Natl. Acad. Sci. USA 2003, 100, 7027–7032.

[38] W. Thies, Fett Wiss. Technol. 1988, 90, 311–314.

[39] S. Chen, B. A. Halkier, Phytochem. Anal. 2000, 11, 174–178.

[40] A. Rykowski, E. Wolinska, H. Van der Plas, J. Heterocycl. Chem. 2000, 37, 879–883.

2.2. Manuscript II

PNAS (2008)

Nonuniform Distribution of Glucosinolates in *Arabidopsis thaliana* Leaves has Important Consequences for Plant Defense

Shroff R*., Vergara F*., Muck A., Svatoš A., and Gershenzon J.

*These two authors have equally contributed to this work.

Max–Planck–Institut für chemische Ökologie

Beutenberg Campus, Hans–Knöll–Str. 8, 07745 Jena

Abstract

The spatial distribution of plant defenses within a leaf may be critical in explaining patterns of herbivory. The generalist lepidopteran larvae, *Helicoverpa armigera* (the cotton bollworm), avoided the midvein and periphery of *Arabidopsis thaliana* rosette leaves and fed almost exclusively on the inner lamina. This feeding pattern was attributed to glucosinolates because it was not evident in a myrosinase mutant that lacks the ability to activate glucosinolate defenses by hydrolysis. To measure the spatial distribution of glucosinolates in *A. thaliana* leaves at a fine scale, we constructed ion intensity maps from MALDI–TOF (matrix assisted laser desorption/ionization–time of flight) mass spectra. The major glucosinolates were found to be more abundant in tissues of the midvein and the periphery of the leaf than the inner lamina, patterns that were validated by HPLC analyses of dissected leaves. In addition, there were differences in the proportions of the three major glucosinolates in different leaf regions. Hence, the distribution of glucosinolates within the leaf appears to control the feeding preference of *H. armigera* larvae. The preferential allocation of glucosinolates to the periphery may play a key role in the defense of leaves by creating a barrier to the feeding of chewing herbivores that frequently approach leaves from the edge.

Introduction

Many plant natural products appear to serve as defenses against herbivores because of their toxicity or deterrence in artificial diets or when added as a supplement to plant material[1, 2]. However, to evaluate the actual defensive role of these substances *in planta*, it is necessary to estimate the amount that a potential herbivore would encounter during feeding. Although determining the amount of plant tissue ingested during a feeding bout is relatively straightforward, measuring the quantity of specific defense products in that tissue is not. Nearly all studies to date have quantified the levels of defensive metabolites at the level of the whole plant or organ[3]. Little is known about the localization of antiherbivore defenses in individual tissues or parts of organs even though this may be critically important to the behavior of small herbivores and to the effectiveness of the defense.

One of the most extensively studied classes of antiherbivore chemical defenses in plants is the glucosinolates, a group of sulfur-rich, amino acid-derived metabolites combining a β–D–glucopyranose residue linked via a sulfur atom to an *N*–hydroxyamino sulfate ester[4] (Fig. 1). Glucosinolates are widespread in the order Capparales, which includes vegetables (cabbage, cauliflower, and broccoli), spice plants supplying condiments (mustard, horseradish, and wasabi), and the model species, *Arabidopsis thaliana*[5, 6]. Upon insect feeding or mechanical disruption, glucosinolates are hydrolyzed by an endogenous glucohydrolase activity known as myrosinase, and the released aglycone rearranges to form isothiocyanates, nitriles, and other products[7] (Fig. 1).
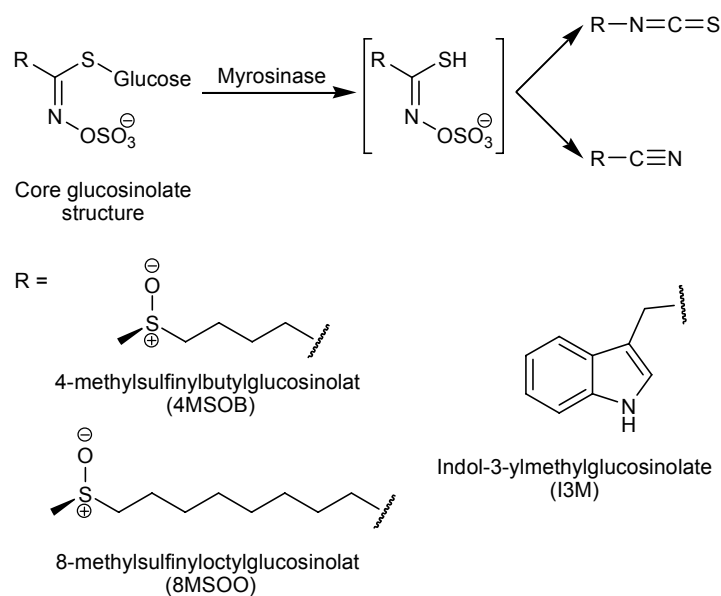
Figure 1. Structures of *Arabidopsis thaliana* glucosinolates identified in this study and scheme for myrosinase catalyzed hydrolysis of glucosinolates to isothiocyanates and nitriles

Nearly all of the defensive properties of glucosinolates can be attributed to the toxicity and deterrence of these hydrolysis products[4]. To avoid premature hydrolysis and autotoxicity, glucosinolates and myrosinase are stored in separate cells or cellular compartments in the plant[8], but these compartments cannot be too far apart or they would not mix together and react efficiently after herbivore damage. Despite the importance of glucosinolate and myrosinase localization in the activation of this defense system, little is known about their locations within individual leaves, stems, or other organs and how this may influence patterns of herbivory. For tissue- or organ-level localization studies, investigators must employ an analytical technique that is sensitive enough for small samples yet specific enough for the compounds of interest. Considering the widespread occurrence of natural products in plants, relatively few suitable histochemical[9], immunocytochemical[10], or spectroscopic techniques[11] have been developed for fine–scale localization in plant tissues. Recently, spectrometric imaging techniques have become available that are capable of mapping metabolite distribution in biological samples with cellular-like resolution[12, 13]. Among these is MALDI–TOF (matrix assisted laser desorption/ionization–time of flight) mass spectrometric imaging that was introduced by Caprioli in 1997[14]. The sample is sprayed with a matrix, and the ions of interest are desorbed from the tissue

by using a conventional MALDI source. The laser position over the target is gradually changed in steps over a predetermined x, y–grid, and the final ion image is plotted by using three–dimensional coordinates with x and y axes for positions and the z axis for the intensity of the particular ion[15]. Diverse analytes have been characterized by MALDI TOF imaging including drugs, peptides, and proteins in animal tissues[16], and herbicides[17] and peptides[18] in plants. However, despite several very recent reports on MALDI imaging of sugars in plants[19, 20], the distribution of secondary natural products in intact plant tissue has not been determined by using mass spectrometric imaging. Moreover, in most cases the distribution of compounds determined by mass spectrometric imaging has not been validated by using independent methods.

Here, we report the fine–scale, spatial distribution of glucosinolates in leaves, as determined by MALDI–TOF imaging of *A. thaliana*, and relate this distribution to the pattern of herbivory caused by larvae of the lepidopteran, *Helicoverpa armigera* (the cotton bollworm). The glucosinolate distribution was confirmed independently by using HPLC and compared with the spatial distribution of myrosinase in the same species. Feeding experiments with *H. armigera* revealed that the relative abundance of glucosinolates in the inner *vs.* the peripheral part of the leaf is significant for insect preference and antiherbivore defense.

Results

***H. armigera* Larvae Avoid the Midvein and Leaf Periphery When Feeding on *A. thaliana* Leaves**

Many small herbivores do not feed uniformly on all parts of the leaf but forage preferentially on specific parts[21]. To study this phenomenon and determine its link to the distribution of plant defenses, we began by making extensive observations of the feeding behavior of first– and second–instar larvae of *H. armigera*, a generalist feeder, on mature rosette leaves of *A. thaliana*. Larvae were found to consistently avoid the periphery of the leaf and the midvein and feed almost exclusively on the inner lamina (Fig. 2). When second–instar *H. armigera* were offered a choice between disks cut from the outer lamina (periphery) and inner lamina, they fed significantly more on the inner lamina (Fig. 3). This preference could be a result of the inner lamina having an increased nutrient content, reduced toughness, or lower levels of glucosinolate defenses.

Figure 2. Feeding pattern of *H. armigera* larvae on mature rosette leaf of *A. thaliana*. Ten second–instar larvae were allowed to feed for 5 h. This photograph is representative of five trials. Photograph by Danny Keßler.
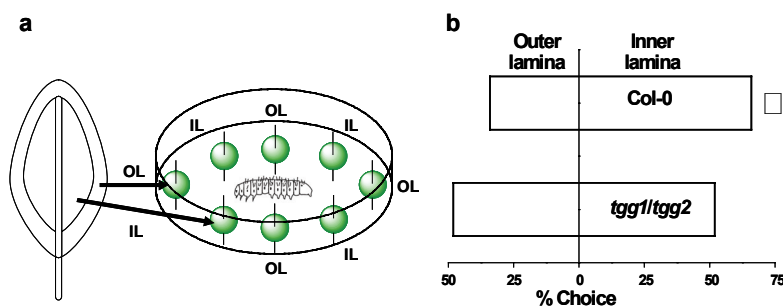
Figure 3. Feeding preference of second–instar *H. armigera* larvae for regions of *A. thaliana* leaves. (a) Bioassay arena in a 10–mm Petri dish equipped with leaf disks from outer lamina (OL) and inner lamina (IL). Leaf disks and caterpillar are not shown to scale. (b) Bioassay results on *A. thaliana* wild type (n = 30) and *tgg1/tgg2* mutant line (n = 25). For wild–type leaves, larvae preferred to feed on disks removed from the inner over the outer lamina (binomial test, P = 0.001). There was no significant preference for the corresponding leaf discs from the *tgg1/tgg2* mutant (binomial test, *p* = 0.764), which has the two principal myrosinase genes knocked out and is thus unable to activate the hydrolysis of glucosinolates.

To determine the role of glucosinolates in this behavior, we repeated the choice test with leaves of the *A. thaliana tgg1/tgg2* mutant line[22], which is knocked out in the genes encoding foliar myrosinases and is thus unable to hydrolyze glucosinolates. Such plants should be identical to wild-type *A. thaliana* but lack the ability to mobilize an active glucosinolate defense. Larvae of *H. armigera* showed no preference for leaf disks cut from the outer *versus* the inner lamina of *tgg1/tgg2* leaves (Fig. 3) suggesting that glucosinolate content is responsible for the choice of feeding site on wild–type plants.

MALDI–TOF Imaging Shows the Highest Glucosinolate Concentrations in Midvein and Leaf Periphery

We investigated the localization of glucosinolates in *A. thaliana* leaves by axial MALDI–TOF imaging of intact leaves that were sprayed on one side with a matrix by using a commercial air brush that provided a very uniform deposition as confirmed by measurement of a matrix ion from an actual leaf sample after coating with matrix (Fig. 4b). Analytes on the leaf maintained their relative position during matrix application and sample evacuation before MALDI measurement (Fig. 4d and e). Negative ion analysis was selected because it should be a more suitable technique for desorption/ionization of anionic species like glucosinolates than positive ion analysis and should yield a spectrum with less noise. The experimental protocol used was very sensitive, yielding mass spectra with very clear signals for the $M^{\ominus}$ ions of glucosinolates from very low amounts of sample. As little as 60 pg of authentic glucosinolate standards provided readily detectable peaks (signal–to–noise ratio of at least 5). The three glucosinolates detected in *A. thaliana* leaves were 4–methylsulfinylbutylglucosinolate (4MSOB, glucoraphanin, *m/z* 436, $M^{\ominus}$), indol–3–ylmethylglucosinolate (I3M, glucobrassicin, *m/z* 447, $M^{\ominus}$) and 8–methylsulfinyloctylglucosinolate (8MSOO, glucohirsutin, *m/z* 492, $M^{\ominus}$) (Fig. 4a). These three compounds are reported to be among the major glucosinolates of *A. thaliana* rosette leaves (Columbia ecotype), together making up >75% of the total glucosinolate composition[23]. The identity of these compounds in the MALDI–TOF mass spectra was confirmed by accurate mass measurement and the isotopic pattern of their respective $M^{\ominus}$ ions. Glucosinolates give a characteristic isotopic pattern with unusually intense A+2 isotope signals because of the presence of two to three sulfur atoms in their structures (Fig. 1). Further confirmation was obtained by comparing CID (collision-induced dissociation) mass spectra of 4MSOB and I3M standards to spectra obtained directly from the leaf [see supporting information (SI) Table S1] acquired by using an atmospheric pressure MALDI source connected to a linear ion trap instrument.
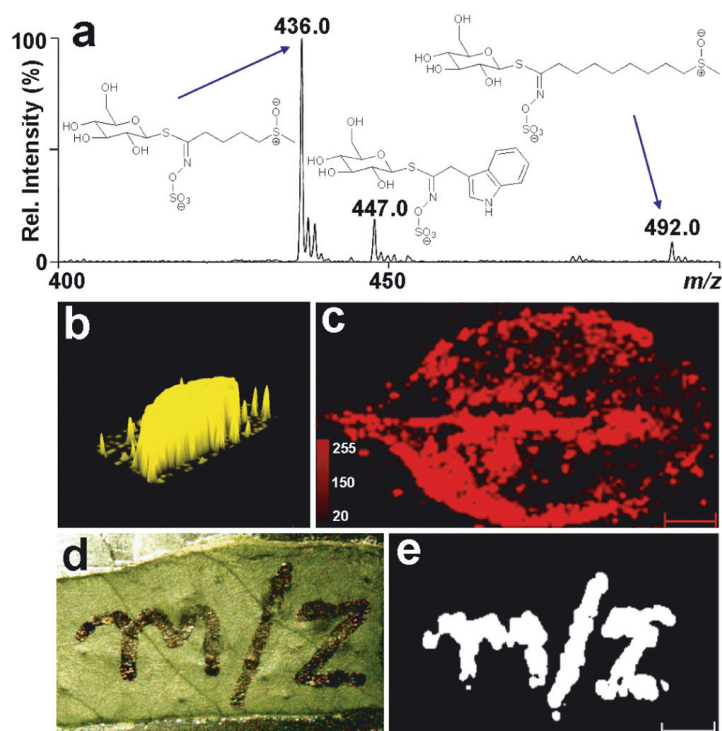
Figure 4. Mass spectrometric imaging of *A. thaliana* leaves. (a) Section (*m/z* 400–500) of a MALDI–TOF/MS spectrum averaged from 100 consecutive pixels on a leaf sprayed on its abaxial side with 9–aminoacridine as a matrix. The molecular peaks at *m/z* 436.0, 447.0, and 492.0 correspond to M$^{\ominus}$ ions of 4–methylsulfinylbutylglucosinolate (4MSOB), indol–3–ylmethylglucosinolate (I3M), and 8–methylsulfinyloctylglucosinolate (8MSOO), respectively. The spectra were collected in a negative reflectron mode on a MALDI micro MX (Waters). (b) Three–dimensional ion intensity map of the matrix ion [*m/z* 193.0 ± 0.25 (M + H)$^{\ominus}$] from measurement of a leaf sample mounted on the MALDI target plate. The image demonstrates that the matrix was deposited homogeneously over the leaf. The spraying area was defined with a paper mask to prevent matrix dispersal during application. (c) Ion intensity map of 4MSOB (*m/z* 436 ± 0.25) created in ImageJ software from ≈100,000 MALDI–TOF/ MS spectra (420 x 252 pixels (w x h), pixel size 200µm). The ion intensities are displayed in a pseudocolor on an intensity scale of 0–255 shades (see inset for the color scale). (d and e) To demonstrate that analytes on the leaf are not delocalized during matrix application and the other steps of sample processing, a permanent marker pen with methanol–soluble ink was used to write "*m/z*" on the leaf. The intensity image of a characteristic ion from the marker ink (*m/z* 663.8) obtained after coating with the 9–aminoacridine matrix corresponds well to the original ink pattern. The matrix coating and the instrumental acquisition parameters were identical to those used in the other imaging experiments. (Scale bars in c and e: 0.5 cm.)

MALDI–TOF spectra were collected from the whole leaf at 200 µm spatial resolution in both *x* and *y* directions (≈100,000 mass spectra per leaf), providing a resolution of 2,500 pixels cm^{-2}. Conversion of the ion chromatogram to ion intensity images showed a distinct, nonuniform distribution of glucosinolates within the leaf. Statistical evaluation indicated that the greatest abundance of glucosinolates was in the midvein and peripheral portions of the leaf lamina. Depicted is a series of five leaves of the basic measurement set (Fig. 5a), plus one larger leaf showing the pattern in more detail (Fig. 4c). For 4MSOB and 8MSOO, significantly greater amounts were present in the midvein compared with the outer and inner leaf lamina (Fig. 6a). On the other hand, I3M exhibited greater abundance in the outer lamina than the inner lamina or midvein.
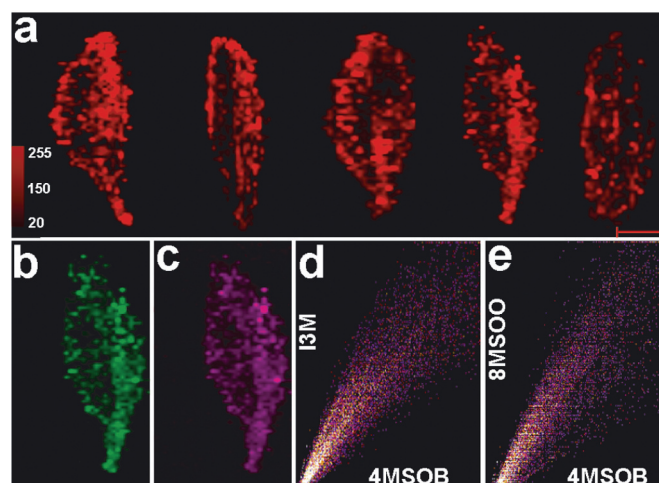

Figure 5. Imaging reveals nonuniform glucosinolate distribution in *A. thaliana* leaves. (a) Five different leaves measured and displayed as in Fig. 2 showing observed 4MSOB ion patterns. (Scale bar: 1 cm.) (b and c) Ion intensity maps of I3M (477 ± 0.25) and 8MSOO (492 ± 0.25), respectively, obtained from mass data measured on the next to last leaf in a. (d) A scatter plot of 4MSOB *vs*. I3M obtained with the ImageJ applet[36]. The correspondence with a line of slope *y* = *x* shows the extent to which the two compounds co–occur. Scales are in false color intensity (0–255) for both *x* and *y* axes. (e) A scatter plot of 4MSOB *vs*. 8MSOO.

HPLC Analyses Confirm the Pattern of Glucosinolate Distribution

To validate the mass spectrometric imaging patterns, glucosinolate analysis of leaf parts was conducted by using an established analytical method, HPLC of the desulfated derivatives with UV detection[23]. The distribution of glucosinolates observed by means of this technique correlated well with the pattern observed by MALDI-TOF imaging. Larger amounts of 4MSOB and 8MSOO were found in the midvein than in other areas of the leaf, and larger amounts of I3M were found in the outer lamina (Fig. 6c). Relative to the other glucosinolates, the signal for I3M was lower in the HPLC analysis than with MALDI–TOF imaging, probably because of the more facile desorption of aromatic glucosinolates by the UV laser compared with glucosinolates with aliphatic side chains; however, the two methods showed very similar trends. The total amount of the three measured glucosinolates was as high in the midvein (which makes up ≈15% of the total leaf area) as in the remainder of the leaf. To determine whether the glucosinolates were colocalized at a small scale, the *x, y* positions of their ion intensity images (Fig. 5a–c) were plotted against each other (Fig. 5d and e). A linear relationship between 4MSOB and I3M and between 4MSOB and 8MSOO was clearly visible indicating a general occurrence of all three glucosinolates at a fine scale throughout the leaf despite differences among them in relative abundance.

The activation of glucosinolates for plant defense requires hydrolysis by myrosinase. Hence, we also investigated the distribution of myrosinase activity in *A. thaliana* leaves. An *in vitro* assay of different leaf parts from 20 leaves showed no significant differences in myrosinase activity among the midvein (4.57 ± 0.844, mean $\pm$ SE in nmol of glucose x mg of leaf^{-1}), outer lamina (4.21 ± 0.622) and inner lamina (4.32 ± 0.957) by ANOVA.
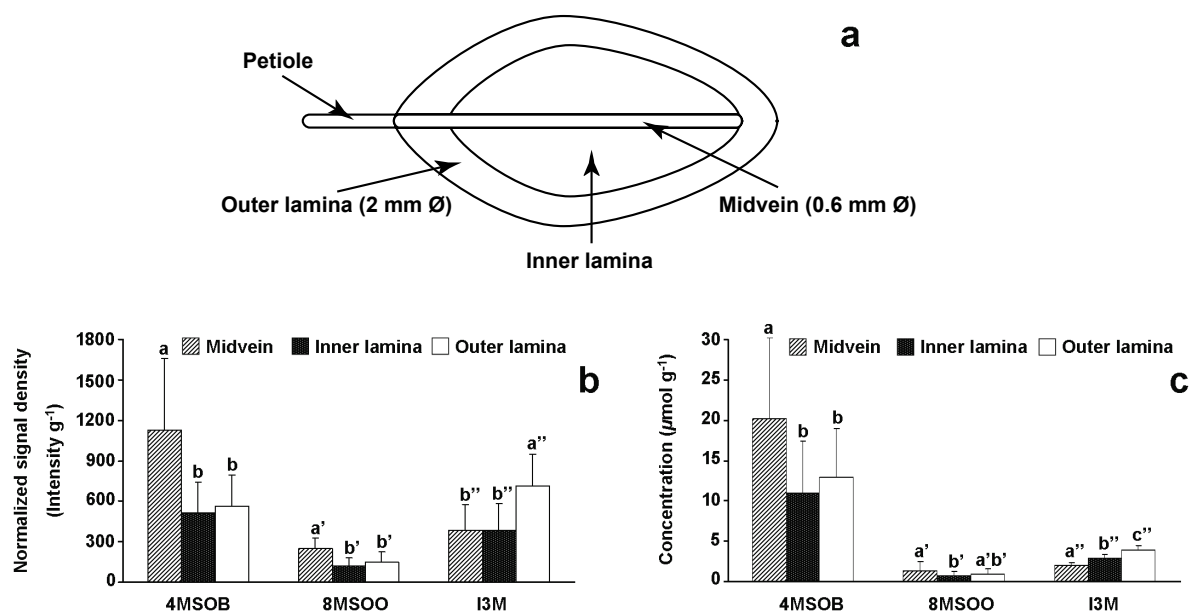
Figure 6. Comparison of the relative amounts of the three measured glucosinolates in three different leaf regions of *A. thaliana* leaves defined as in a. Normalized ion intensities were calculated for the midvein, the inner lamina, and the outer lamina areas from mass spectrometric imaging (b) and glucosinolate concentrations were measured by HPLC analysis (c). Error bars represent SEM from five mature leaves from different plants. Bars marked by different letters show significant difference at $p < 0.05$.

Discussion

Ion intensity maps constructed from MALDI–TOF mass spectra demonstrated that glucosinolates have a nonuniform distribution in the leaves of *A. thaliana*. Of the three major glucosinolates analyzed, two were more abundant in the midvein than the rest of the leaf, whereas one was more abundant on the edge of the leaf than elsewhere. These results were confirmed by HPLC analysis. The protocol used represents an advance over existing mass spectrometric imaging methods by allowing very sensitive measurements of metabolite distribution in an intact leaf in a quantitative manner that can be statistically analyzed and validated by independent methods.

The nonuniform distribution of glucosinolates in *A. thaliana* leaves appears to explain the feeding preference of *H. armigera* larvae for specific portions of the leaf. In whole–leaf trials and leaf disk bioassays, larvae avoided feeding on the midvein and the edge of the leaf, the locations with high levels of glucosinolates. Furthermore, this preference hierarchy was not evident during feeding on *tgg1*/*tgg2* mutants, which lack foliar myrosinases and so are unable to activate their glucosinolate defenses. The glucosinolates in *A. thaliana* leaves are deployed such that the greatest concentrations are present in the midvein and leaf periphery. This pattern may result from various physiological constraints on the synthesis and storage of glucosinolates in certain tissues. For example, the formation of glucosinolates might occur only in vascular bundles because certain biosynthetic enzymes are restricted to this tissue[24, 25]. Storage may only be possible in certain parts of the leaf because of the need to avoid autotoxicity to sensitive cells.

The nonuniform distribution of glucosinolates is also likely to have ecological significance because, like other plants, *A. thaliana* may have been selected to maximize its antiherbivore defenses at sites that are most valuable or vulnerable to attack[26]. The midvein is critical to the function of the leaf because damage to this structure would disrupt the transport of water and nutrients and assimilate throughout the leaf. In addition, the integrity of the periphery may also be vital for leaf function because this tissue stabilizes leaf architecture even if there is damage to the inner parts. The high concentration of defenses on the leaf periphery may function as a barrier to insect herbivores that initiate feeding from the leaf edge, a behavior often

observed for older instars of *H. armigera* and other lepidopteran species (F.V., unpublished results).

The distribution of defense compounds in leaves is not often studied at a scale relevant to small herbivores, but in previous work, certain other defense compounds have been localized in peripheral tissues. For example, cyanogenic glycosides are localized in the epidermal cells of sorghum[27], monoterpenes and diterpenes are found in glandular hairs projecting from the epidermis of many members of the Lamiaceae[28], and higher terpenes form a surface resin on leaves of Newcastelia viscida[29]. Glucosinolate distribution within leaves was the subject of previous work as well, at a much coarser scale of analysis than in the present study. Wild radish leaves were shown to have higher concentrations of glucosinolates in their lower halves than in their distal halves with a high degree of random variation[30].

The localization of plant glucosinolates at the cellular level is also poorly investigated with the exception of a report that glucosinolates in *A. thaliana* flower stalks are found in elongated cells just outside the vascular system and adjacent to the phloem[31]. As mentioned above, the transcripts of glucosinolate biosynthetic genes have also been associated with vascular tissues[24, 25]. Our measurements of high glucosinolate content in the midvein support the association of glucosinolate storage with the vascular system. However, the diffuse localization we observed throughout the leaf lamina suggests that much of the stored glucosinolate pool is not associated with vascular tissue.

An aspect of glucosinolate localization in plants that has been controversial in recent years is whether or not these compounds are found on the leaf surface[32, 33]. The presence of glucosinolates on the surface would supply important cues for insect host choice. In our work, we found it necessary to spray many coats of matrix (15 coats) to achieve reproducible imaging, suggesting that glucosinolates in *A. thaliana* leaves are not very abundant on the surface. When standard glucosinolates were applied directly to the leaf surface, clear spectra were noted after only one to two coatings of matrix. Further information on the vertical distribution of glucosinolates in the leaf was not readily apparent from our results. In contrast to glucosinolates, much more is known about the cell– and organ–level localization of myrosinase. This glucosinolate–activating enzyme is known from all plant organs[4], and in *A. thaliana* is reported from the phloem parenchyma as well as guard cells[34, 35]. Unlike

glucosinolates, we found myrosinase activity to be uniformly distributed among the different sectors of the leaf examined.

In summary, MALDI–TOF imaging of *A. thaliana* leaves has revealed a distinctive pattern of glucosinolate distribution that has important implications for the feeding of a generalist lepidopteran larva. Further investigation of the distribution of glucosinolates and other defensive metabolites in plant tissue should help evaluate their defensive roles and reveal how plants have been selected to deploy defenses for maximum benefit.

Materials and Methods

Detailed descriptions of chemicals, plants, and insects used together with further details on MS imaging, HPLC analyses and myrosinase assays are given in SI Text.

Insect Feeding Experiments

H. armigera (Lepidoptera: Noctuidae) were grown on an artificial pinto bean-based diet[36] and used at the second-instar stage. Larvae were not fed the previous 12 h before beginning experiments. For whole–leaf tests, single larvae were placed randomly on mature 4–week–old *A. thaliana* Columbia ecotype or *tgg1/tgg2* rosette leaves that had been freshly removed from the plant and placed with the petiole in water. The location of feeding damage was recorded after 5 h. For leaf disk tests, 2–mm–diameter disks of *A. thaliana* Columbia ecotype or *tgg1/tgg2* leaves were removed either from the outer lamina (2–mm–wide strip on periphery) or inner lamina (remaining leaf excluding midvein) by using a hole punch. Plastic Petri dishes were filled with agar (2% wt/vol, 5 mm height) and the disks suspended 2–3 mm above the solidified agar surface by using entomological pins. Four outer and four inner lamina disks from the same leaf were placed alternately along the edge of each Petri dish (Fig. 3a). A single larva was then placed with a random orientation in the center of each dish. After it had fed for 10 consecutive seconds on a single disk, the type of the disk was recorded. Results were analyzed by a binomial test.

Leaf Preparation for Imaging

Solutions of 9–aminoacridine free base[37] were prepared at 15 mg mL^{-1} in HPLC–grade methanol. The leaves were mounted on a MALDI stainless steel LockMass target plate (LM; Waters) by using a doublesided adhesive tape with the abaxial surface of the leaf facing up. After mounting, leaves were spray–coated with 9–aminoacridine by using a commercial airbrush with a 0.2–mm–diameter sprayer jet. The target plate was kept at a 45° angle against a plastic support and the sprayer held at a distance of 13 cm from the plate. This insured that the cone of the spray reaching the target covered the entire leaf. Each coating involved 20–22

seconds of spraying, followed by 5 min of drying. This process was typically carried out 15 times to give maximal signal strength. Mass spectrometric imaging was primarily done with the abaxial side of the leaf up because this side offered a better surface for uniform matrix deposition owing to fewer trichomes; however, the same pattern of glucosinolate distribution was observed when imaging was carried out on the adaxial side. Detailed descriptions of chemicals, plants, and insects used together with further details on MS imaging, HPLC analyses and myrosinase assays are given in SI Text.

Mass Spectrometry

A MALDI microMXmass spectrometer (Waters) fitted with a nitrogen laser (337–nm, 4–ns laser pulse duration, 10 Hz, and 154 μJ per pulse) was used in a reflectron mode and negative polarity for data acquisitions by using MassLynx version 4.0 software. The x, y coordinates for the imaging acquisition were defined by using proprietary software. The chemical identity of the compounds encountered was confirmed by mass spectrometry on an LTQ ion trap instrument (Thermo Fisher) with an AP–MALDI source equipped with a solid-state NdYAG UV laser (MassTech) and running Target 6 (MassTech) and Excalibur v.2.0 (Thermo Fisher) software for data acquisition.

Construction and Quantification of Mass Spectrometric Images

Spectral data for the respective molecular ions of the three glucosinolates, 4–methylsulfinylbutylglucosinolate (*m/z* 436), indol–3–ylmethylglucosinolate (*m/z* 447), and 8–methylsulfinyloctylglucosinolate (*m/z* 492), were exported in the software ImageJ (http://rsb.info.nih.gov/ij/) for converting them into two-dimensional ion intensity maps. Ion maps were constructed by using a ± 0.25 Da mass window, because the roughness of the leaf surface could reduce mass accuracy. Each image was first desaturated by using ImageJ software and then divided into regions as in Fig. 6a. The outer lamina was defined as a 10–pixel (2 mm) –wide region around the periphery of the leaf, the midvein as a 3–pixel (0.6 mm)–wide region around the midvein and the remaining leaf was defined as the inner lamina for quantitation. The signal densities (D) of the respective leaf regions (AR in pixels) were integrated, normalized against the dry weight of each leaf (DW in g) by using total leaf area (AT

in pixels), and plotted as normalized signal intensities (NSI) according to the following formula: NSI = D/(AR/AT x DW).   Results from eight leaves were analyzed by conducting a one–way ANOVA, followed by a Tukey post hoc test using SPSS v15 software. For 4MSOB, the midvein showed a significant difference from the inner (P = 0.007) and outer (P = 0.014) lamina.   For I3M, the outer lamina showed a significant difference from the inner lamina (P = 0.015) and midvein (P = 0.014). The 8MSOB showed a similar trend as 4MSOB, with the amount in midvein being significantly different from the inner lamina (P = 0.002) and the outer lamina (P = 0.010). The other comparisons among leaf regions for the three glucosinolates were not significant.

HPLC Analysis

Leaves were detached from the plant, flash–frozen in liquid nitrogen, and lyophilized. The freeze–dried leaves were dissected into midvein, outer lamina, and inner lamina (Fig. 6a), and each part was weighed before being individually immersed in tubes set up in a 96–well–plate format filled with 1 mL of methanol containing 0.05 µmol of p–hydroxybenzylglucosinolate as an internal standard. Each tube contained three metallic spheres to grind up the leaf material when the plate was agitated at ≈1,000 rpm on a SO–10m paint shaker for 4 min.   The ground suspensions were centrifuged at 4,200g for 10 min and the supernatants transferred into columns filled with 20 mg of DEAE–Sephadex equilibrated with 800 µL of water, followed by 500 µL of 80% methanol. After 600 µL of sample were loaded, each column was eluted with 500 µL of 80%methanol, 500 µL of water, and 500 µL of 0.02 M Mes buffer (pH 5.2). Next, 25 µL of sulfatase solution [prepared as described[38]] were added to each column and the sample incubated overnight. The resulting desulfoglucosinolates were eluted with 500 µL of water and concentrated for HPLC–DAD (HP–1100 series; Agilent Technologies) analysis as described[3].

Myrosinase Enzyme Assays

Myrosinase activity was quantified by using a modification of a reported method[3].

Acknowledgments

Bibliography

[1] Gershenzon J, Dudareva N (2007) The function of terpene natural products in the natural world. Nat Chem Biol 3: 408–414.

[2] Rosenthal G, Berenbaum M, eds (1992) Herbivores: Their Interactions with Secondary Plant Metabolites (Academic, San Diego), 2nd Ed, Vol 1.

[3] Burow M, Müller R, Gershenzon J, Wittstock U (2006) Altered glucosinolate hydrolysis in genetically engineered *Arabidopsis thaliana* and its influence on the larval development of *Spodoptera littoralis*. J Chem Ecol 32: 2333–2349.

[4] Halkier B, Gershenzon J (2006) Biology and biochemistry of glucosinolates. Ann Rev Plant Biol 57: 303–333.

[5] Fahey JW, Zalcmann AT, Talalay P (2001) The chemical diversity and distribution of glucosinolates and isothiocyanates among plants. Phytochemistry 56: 5–51.

[6] Reichelt M, et al. (2002) Benzoic acid glucosinolate esters and other glucosinolates from *Arabidopsis thaliana*. Phytochemistry 59: 663–671.

[7] Bones AM, Rossiter JT (2006) The enzymic and chemically induced decomposition of glucosinolates. Phytochemistry 67: 1053–1067.

[8] Rask L, et al. (2000) Myrosinase: Gene family coevolution and herbivore defense in Brassicaceae. Plant Mol Biol 42: 93–113.

[9] Eisner T, Eisner M, Meinwald J (1987) Technique for visualization of epidermal glandular structures in plants. J Chem Ecol 13: 943–946.

[10] Peumans W, Hause B, Van Damme E (2000) The galactose–binding and mannosebinding jacalin–related lectins are located in different sub-cellular compartments. FEBS Lett 477: 186–192.

[11] Osbourn A, Clarke B, Lunness P, Scott P, Daniels M (1994) An oat species lacking avenacin is susceptible to infection by *Gaeumannomyces graminis* var. tritici. Physiol Mol Plant Pathol 45: 457–467.

[12] Cooks R, Ouyang Z, Takats Z, WisemanJ (2006) Ambient mass spectrometry. Science 311: 1566–1570.

[13] Ratcliffe RG, Shachar–Hill Y (2001) Probing plant metabolism with NMR. Annu Rev Plant Physiol Plant Mol Biol 52: 499–526.

[14] Caprioli R, Farmer T, Gile J (1997) Molecular imaging of biological samples: Localization of peptides and proteins using MALDI-TOF MS. Anal Chem 23: 4751–4760.

[15] Rubakhin S, Jurchen J, Monroe E, Sweedler J (2005) Imaging mass spectrometry: Fundamentals and applications to drug discovery. Drug Discovery Today 10: 823–837.

[16] Reyzer ML, Caprioli RM (2007) MALDI–MS–based imaging of small molecules and proteins in tissues. Curr Opin Chem Biol 11: 29–35.

[17] Mullen A, Clench M, Crosland S, Sharples K (2005) Determination of agrochemical compounds in soya plants by imaging matrix–assisted laser desorption/ionisation mass spectrometry. Rapid Commun Mass Spectrom 19: 2507–2516.

[18] Kondo T, S Shinichiro, Kinoshita A, Mizuno S, Kakimoto T, Fukuda H, and Sakagami Y (2006) A plant peptide encoded by CLV3 identified by in situ MALDI–TOF MS analysis. Science 313: 845–848.

[19] Li Y, Shrestha B, Vertes A (2007) Atmospheric pressure molecular imaging by infrared MALDI mass spectrometry. Anal Chem 79: 523–532.

[20] Robinson S, Warburton K, Seymour M, Clench M, Thomas–Oates J (2007) Localization of water–soluble carbohydrates in wheat stems using imaging matrix–assisted laser desorption ionization mass spectrometry. New Phytol 173: 438–444.

[21] Schiers J, de Bruyn L, Verhagen R (2001) Nutritional benefits of the leaf–mining behavior of two grass miners: A test of the selective feeding hypothesis. Ecol Entomol 26: 509–516.

[22] Barth C, Jander G (2006) Arabidopsis myrosinases TGG1 and TGG2 have redundant function in glucosinolate breakdown and insect defense. Plant J 46: 549–562.

[23] Brown P, Tokuhisa J, Reichelt M, Gershenzon J (2003) Variation of glucosinolate accumulation among different organs and developmental stages of *Arabidopsis thaliana*. Phytochemistry 62: 471–481.

[24] Reintanz B, et al. (2001) bus, a bushy Arabidopsis CYP79F1 knockout mutant with abolished synthesis of short–chain aliphatic glucosinolates. Plant Cell 13: 351–367.

[25] Schuster J, Knill T, Reichelt M, Gershenzon J, Binder S (2006) Branched-chain aminotransferase 4 is part of the chain elongation pathway in the biosynthesis of methionine–derived glucosinolates in Arabidopsis. Plant Cell 18: 2664–2679.

[26] Hamilton J, Zangerl A, DeLucia E, Berenbaum M (2001) The carbon–nutrient balance hypothesis: Its rise and fall. Ecol Lett 4: 86–95.

[27] Kojima M, Poulton J, Thayer S, Conn E (1979) Tissue distributions of dhurrin and of enzymes involved in its metabolism in leaves of *Sorghum bicolor*. Plant Physiol 63: 1022–1028.

[28] Siebert D (2004) Localization of salvinorin A and related compounds in glandular trichomes of the psychoactive sage *Salvia divinorum*. Ann Bot 93: 763–771.

[29] Dell B, McComb A (1975) Glandular hairs, resin production, and habitat of *Newcastelia viscida* E. Pritzel (Dicrastylidaceae). Aust J Bot 23: 373–390.

[30] Shelton AL (2005) Within–plant variation in glucosinolate concentrations of *Raphanus sativus* across multiple scales. J Chem Ecol 31: 1711–1732.

[31] Koroleva OA, et al. (2000) Identification of a new glucosinolate–rich cell type in Arabidopsis flower stalk. Plant Physiol 124: 599–608.

[32] Griffiths DW, et al. (2001) Identification of glucosinolates on the leaf surface of plants from the Cruciferae and other closely related species. Phytochemistry 57: 693–700.

[33] Reifenrath K, Riederer M, Müller C (2005) Leaf surface wax layers of Brassicaceae lack feeding stimulants for *Phaedon cochleariae*. Entomol Exp Appl 115: 41–50.

[34] Andreasson E, Jorgensen L, Hoglund A, Rask L, Meijer J (2001) Different myrosinase and idioblast distribution in Arabidopsis and *Brassica napus*. Plant Physiol 127: 1750–1763.

[35] Thangstad O, Gilde B, Chadchawan S, Seem M, Husebye H, Bradley D, Bones A (2004) Cell specific, cross-species expression of myrosinases in *Brassica napus*, *Arabidopsis thaliana* and *Nicotiana tabacum*. Plant Mol Biol 54: 597–611.

[36] Joyner K, Gould F (1985) Developmental consequences of cannibalism in *Heliothis zea* (Lepidoptera, Noctuidea). Ann Entomol Soc Am 78: 24–28.

[37] Albert A, Ritchie B (1955) 9-Aminoacridine. Org Synth Coll 3: 53.

[38] Graser G, Oldham NJ, Brown PD, Temp U, Gershenzon J (2001) The biosynthesis of benzoic acid glucosinolate esters in *Arabidopsis thaliana*. Phytochemistry 57: 23 32.

Supporting Information

SI Text

Chemicals

All chemicals were obtained from Sigma–Aldrich unless otherwise stated. The free base of 9–aminoacridine was prepared from the commercially available hydrochloride[1]. Plant Material. Mature leaves from 4–week–old, rosette–stage *Arabidopsis thaliana* of the Columbia accession (Col-0) were used in all experiments. Plants were grown in a soil/vermiculite mixture (3:1) in a controlled environment chamber at 21°C, 55% relative humidity, 100 µmol m^{-2} s^{-1} photosynthetically active radiation from a mixture of Fluora and Cool White lamps (Osram), and a diurnal cycle of 10 h light and 14 h dark.

Leaf Preparation for Imaging

Solutions of 3–aminoquinoline and 9–aminoacridine free bases were prepared at 30 mg mL^{-1} and 15 mg mL^{-1}, respectively, in HPLC–grade methanol. The leaves were mounted on a MALDI stainless steel LockMass target plate (LM; Waters) by using a double–sided adhesive tape with the abaxial surface of the leaf facing up. After mounting, leaves were spray–coated with 3–aminoquinoline or 9–aminoacridine by using a commercial airbrush with a 0.2–mm–diameter sprayer jet. The target plate was kept at a 45° angle against a plastic support and the sprayer held at a distance of 13 cm from the plate. This insured that the cone of the spray reaching the target covered the entire leaf. Each coating involved 20–22 seconds of spraying, followed by 5 min of drying. This process was typically carried out 15 times to give maximal signal strength. The interval between consecutive sprays insured negligible solvent build-up on the leaf which was essential to prevent analyte delocalization. Although a previous report on the use of 3–aminoquinoline as a MALDI matrix for glucosinolate analysis[2] was the starting point for these experiments, 9–aminoacridine[3] was selected eventually as a better matrix because of its ability to more efficiently extract glucosinolates from leaf tissues when applied as a methanolic solution, which is a likely consequence of its smaller crystal size and stronger basicity (pK=4.91 *vs.* 9.96)[4]. Mass spectrometric imaging was primarily done with the abaxial side of the leaf up because this side offered a better surface for uniform matrix

deposition owing to fewer trichomes; however, the same pattern of glucosinolate distribution was observed when imaging was carried out on the adaxial side.

Mass Spectrometry

A MALDI micro MX mass spectrometer (Waters) fitted with a nitrogen laser (337–nm, 4–ns laser pulse duration, max 290 µJ per laser pulse, max 20–Hz repetition rate) was used in a reflectron mode and negative polarity for data acquisitions. The instrument operated with voltages of 5 kV on the sample plate, 12 kV on the extraction grid and pulse and detector voltages of 2.2 kV and 2.35 kV, respectively. The laser frequency and energy were optimized for glucosinolates at 10 Hz and 154 µJ per pulse. The matrix-sprayed leaves fixed to a metallic LM plate were introduced at the source and evacuated for ca 5 h. MassLynx v4.0 software (Waters) was used for data acquisition and each spectrum was recorded at 10 laser pulses. The x, y coordinates for the imaging acquisition were defined using proprietary software. PEG 600 sulfate was used to calibrate the mass spectrometer for a mass range of 100–1,000 Da. The chemical identity of the compounds encountered was confirmed by mass spectrometry on an LTQ ion trap instrument (Thermo Fisher) with an AP–MALDI source equipped with a solid–state NdYAG UV laser and running Target 6 (MassTech) and Excalibur v.2.0 (Thermo) software for data acquisition.

HPLC Analysis

Leaves were detached from the plant, flash-frozen in liquid nitrogen, and lyophilized. The freeze–dried leaves were dissected into midvein, outer lamina, and inner lamina (Fig. 6a), and each part was weighed before being individually immersed in tubes set up in a 96–well–plate format filled with 1 mL of methanol containing 0.05 µmol of p–hydroxybenzylglucosinolate as an internal standard. Each tube contained three metallic spheres to grind up the leaf material when the plate was agitated at ≈1,000 rpm on a SO–10m paint shaker for 4 min. The ground suspensions were centrifuged at 4,200g for 10 min, and the supernatants were transferred into columns filled with 20 mg of DEAE–Sephadex equilibrated with 800 µL of water, followed by 500 µL of 80% methanol. After 600 µL of sample were loaded, each column was eluted with 500 µL of 80% methanol, 500 µL of water, and

500 µL of 0.02 M Mes buffer (pH 5.2). Next 25 µL of sulfatase solution [prepared as described[5]] were added to each column and the sample incubated overnight. The resulting desulfoglucosinolates were eluted with 500 µL of water and concentrated for HPLC-DAD (HP–1100 series; Agilent Technologies) analysis employing a Lichrospher 100 RP-18 (250 x 4.6 mm; WiCom) column with the following gradient of water (solvent A) and acetonitrile (solvent B) at a flow rate of 1 ml min^{-1}: 1.5–5% (vol/vol) B (6 min), 5–7% (vol/vol) B (2 min), 7–21% (vol/vol) B (10 min), 21–29% (vol/vol) B (5 min), 29–100% (vol/vol) B (30 s), 100% B (2 min 30 s), 100–1.5% (vol/vol) B (6 s), 1.5% B (4.54 s). Chromatograms were recorded at 229 and 280 nm and UV spectra acquired between 190 and 360 nm.

Myrosinase Enzyme Assays

Myrosinase activity was quantified by using a modification of a previously reported method[6]. Briefly, crude plant extracts were prepared by grinding the leaf material with 150 µL of 50 mM Mes buffer (pH 6.0). After incubation at room temperature for 5 min, samples were centrifuged at 10,000g for 10 min. Assays were carried out with 1 mM allylglucosinolate and 75 µL of plant extract in a total volume of 100 µL. After incubation at 37°C for 30 min, the reaction was stopped by boiling (95°C for 5 min). Samples were centrifuged at 10,000g for 5 min, and 90µL of the supernatant were used for glucose determination by using a Glucose GOD/ PAP kit (Randox). Absorbance was measured at 500 nm, and the amount of glucose formed by myrosinase was calculated based on a calibration curve obtained from measurement of glucose standards. These values were then adjusted by subtraction of endogenous glucose measured in assays without added allylglucosinolate. Results were analyzed by ANOVA.

Bibliography

[1] Albert A, Ritchie B (1955) 9–Aminoacridine. Org Synth Coll 3: 53.

[2] Botting C, Davidson N, GriffithsD, Bennett R, Botting N (2002) Analysis of intact glucosinolates by MALDI–TOF mass spectrometry. J Agric Food Chem 50: 983–988.

[3] Shroff R, Muck A, Svatos A (2007) Analysis of low molecular weight acids by negative mode MALDI–TOF/MS. Rapid Commun Mass Spectrom 21: 3295–3300.

[4] Perrin D (1965) Dissociation Constants of Organic Bases in Aqueous Solution, (Butterworth, London).

[5] Graser G, Oldham N, Brown P, Temp U, Gershenzon J (2001) The biosynthesis of benzoic acid glucosinolate esters in *Arabidopsis thaliana*. Phytochemistry 57: 23–32.

[6] Burow M, Müller R, Gershenzon J, Wittstock U (2006) Altered glucosinolate hydrolysis in genetically engineered Arabidopsis thaliana and its influence on the larval development of *Spodoptera littoralis*. J Chem Ecol 32: 2333–2349.

Table S1. Identification of principal glucosinolates of *A. thaliana* leaves observed in mass spectrometric imaging by collision–induced dissociation (CID)

Molecular peak	CID spectrum	CID standard	Identification
436	436 [$M^{\ominus}$], 372 (bp), 259	436 [$M^{\ominus}$], 372 ($M^{\ominus}$ –$CH_3SH(O)$, bp), 259	4–methylsulfinylbutylglucosinolate
447	447 [$M^{\ominus}$], 367, 311, 291, 275, 259 (bp), 241, 205	447 [$M^{\ominus}$], 367, 311, 291, 275, 259 (bp), 241, 205	Indol–3–ylmethylglucosinolate
492	492 [$M^{\ominus}$], 428 ($M^{\ominus}$ –$CH_3SH(O)$, bp), 229, 259	na	8–methylsulfinyloctylglucosinolate

na, not available; bp, base peak.

2.3. Manuscript III

In Preparation

Determination of the Absolute Configuration of the Glucosinolate Methyl Sulfoxide Group
Reveals a Stereospecific Biosynthesis of the Side Chain

Fredd Vergara[1]*, Michael Wenzler[1]*, Bjarne G. Hansen[2], Daniel J. Kliebenstein[3], Barbara A. Halkier[2], Jonathan Gershenzon[1], and Bernd Schneider[1]

*These two authors have equally contributed to this project.
[1]Max–Planck–Institute for Chemical Ecology,
Beutenberg Campus, Hans–Knöll–Straße 8, D–07745 Jena, Germany
[2]Plant Biochemistry Laboratory, Department of Plant Biology, Faculty of Life Sciences, University of Copenhagen, DK–1871 Frederiksberg C, Denmark
[3]University of California–Davis, Department of Plant Sciences, Mail Stop 3, One Shields Ave, Davis, CA 95616-8780 USA

Abstract

Glucosinolates are plant metabolites containing an anionic nitrogeneous thioglucosidic core structure and a structurally diverse amino acid-derived side chain, which after hydrolysis by thioglucohydrolases (myrosinases) afford biological active degradation products such as nitriles and isothiocyanates. Structural diversity in glucosinolates is partially due to enzymatic modifications occurring on the preformed core structure, like the recently described oxidation of thioethers to sulfoxides catalyzed by a flavin monooxygenase identified in *Arabidopsis thaliana*. The enzyme product, 4–methylsulfinylbutylglucosinolate, bears a chiral sulfoxide group in its side chain. We have analyzed the epimeric purity of 4–methylsulfinylbutylglucosinolate by NMR methods using a chiral lanthanide shift reagent. The absolute configuration of the sulfoxide group has been established by comparing the ^{1}H NMR spectra of the two sulfoximine diastereomers of natural 4–methylsulfinylbutylglucosinolate. According to our data, 4–methylsulfinylbutylglucosinolate isolated from broccoli and *A. thalia*na is a pure epimer and its sulfoxide group has the R_S configuration. The product of the *A. thaliana* flavin monooxygenase has these same properties demonstrating that the enzyme is stereospecific and supporting its involvement in glucosinolate side chain formation.

Introduction

Glucosinolates are plant metabolites defined by the presence of a core structure, containing a β–D–thioglucopyranose residue and a *N*–hydroxyiminosulfate ester, which is linked to a variable side chain. More than a hundred glucosinolates have been described (Halkier and Gershenzon, 2006) and part of this structure diversity arises from secondary modifications carried out on the core structure. 4–Methylsulfinylbutylglucosinolate (glucoraphanin, **1**, Fig. 1) is an abundant glucosinolate in the commercially important crops of the genus *Brassica* (broccoli, cabbage) as well as in the Col–0 accession of the model plant *Arabidopsis thaliana* (Fahey et al., 2001) of the Brassicales order. The biosynthesis of aliphatic glucosinolates like **1** is conceptually divided in three phases starting from methionine; first, the amino acid chain is elongated; second, the core structure is formed; and third, the aliphatic chain undergoes secondary modifications (Halkier and Gershenzon, 2006). An example of a secondary modification is the conversion of **3** to **1** (Fig. 2), which involves the oxidation of the thiol residue to a sulfoxide group. Such sulfoxide groups are found in many glucosinolates (Fahey et al., 2001).
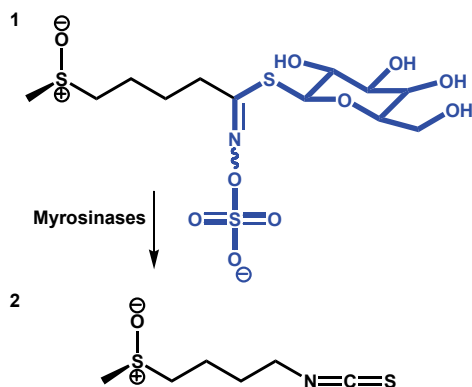
Figure 1. *Hydrolysis of glucosinolates*. Plants of the Brassicaceae produce glucosinolates, such as 4–methylsulfinylbutylglucosinolate (**1**). After tissue damage the enzyme myrosinase hydrolyzes the glucosinolates to products including isothiocyanates, such as sulforaphane (**2**), which is a chiral molecule due to the presence of the asymmetric sulfoxide group. The core structure common to all glucosinolates is shown in **1** with bold (blue) bonds.

X–ray analyses have shown that sulfoxides have a trigonal pyramidal geometry (Carey et al., 1976; Kodama et al., 1976). Because their pyramidal inversion barrier typically is in the range of 35–43 kcal mol^{-1} (Bentley 2005), stable sulfoxide enantiomers are possible if $R_1 \neq R_2$, as in **1**. However, the stereochemistry of the sulfoxide moiety of glucosinolates is rarely considered although its configuration may be critical for its biological activity and the biological activity of glucosinolate hydrolysis products formed by myrosinase catalysis following plant damage (Halkier and Gershenzon, 2006). In the case of **1**, its myrosinase–mediated hydrolysis product, sulforaphane (**2**, Fig. 1) has been intensively investigated for its anticancer activity, attributable to its ability to modulate phase I and phase II detoxification pathways (Fimognari and Hrelia, 2007). Nevertheless only one study has evaluated the influence of the stereochemistry of the sulfoxide group of **2** on its anticancer activity (Zhang and Tang, 2007).

Sulfur chirality has not been as widely addressed as carbon chirality in natural products and medicinal chemistry. Nevertheless, there are some illuminating examples that demonstrate the relevance of sulfoxide stereochemistry to biological activity. For instance, $S_C S_S$– but not $S_C R_S$–methionine sulfoxide was recognized by the enzyme gamma-glutamyl transpeptidase, responsible for the transfer of a gamma–glutamyl moiety from a donor substrate to acceptors, such as amino acids and water (Lherbet and Keillor, 2004). In addition, the S_S enantiomers of hexyl methyl sulfoxide and methyl phenyl sulfoxide bound more tightly (about 5–8–fold) than the R_S enantiomers to horse liver alcohol dehydrogenase (Cho and Plapp, 1998). A drug called Nexium$^{®}$ (esomeprazole, that is the pure S_S isomer), is often prescribed instead of the racemic mixture, Prilosec$^{®}$ (Losec$^{®}$, omeprazole), owing to its better clinical properties as a proton pump inhibitor (Olbe et al., 2003).

Knowledge about the epimeric purity and configuration of the glucosinolate side chain sulfoxide moiety would also shed light on the specificity of glucosinolate biosynthetic enzymes. The *S*–oxidation of methylthioalkyl glucosinolates leading to the formation of the sulfoxide in **1** is carried out by a flavin monooxygenase (FMO) encoded by the gene *FMO$_{GS-OX1}$* (*At1g65860*) recently identified in *A. thaliana* using a combination of *in silico* and biochemical data (Hansen et al., 2007). But, it is not known if this enzyme produces a chiral sulfoxide, and if so which configuration.

The enantiomeric purity of some sulfoxides has been determined using chiroptical methods or chiral chromatography, while their absolute configuration has

been determined via X–ray crystallography, nuclear magnetic resonance (NMR) spectroscopy and chiroptical methods like optical rotatory dispersion (ORD) and circular dichroism (CD) (Donnoli et al., 2006). To date no study has reported on the epimeric purity or the absolute configuration of sulfoxides in intact glucosinolates. However, the combination of ORD and X–ray data showed that the glucosinolate hydrolysis product **2** isolated from several plant sources is an optically active compound with the R_S absolute configuration (Mislow et al., 1964; Cheung et al., 1965), but nothing is known about sulfoxide-containing glucosinolates nor about the stereospecificity of the sulfoxides produced by the flavin monooxygenase enzyme, (*At1g65860*).

In this investigation, we set out to develop an accurate, sensitive method to determine the stereochemistry of the sulfoxide group of glucosinolate side chains that could be applied to plant metabolites or the products of an enzyme assay. Chiral HPLC and chiroptical methods tested failed to determine the epimeric purity of glucosinolates at their sulfoxides, most probably because additional stereocenters also interacted with the stationary phase or the absorption spectrum was dominated by other functional groups in the molecule, respectively. Hence we turned to NMR using a chiral lanthanide shift reagent (CLSR) which relies on the anisotropy generated by europium to resolve signals for epimers. The absolute configuration of the sulfoxide in glucosinolate side chains was assessed via an extension of the Mosher method by preparing the *N*–(methoxyphenylacetyl)sulfoximine derivative according to Yabuuchi et al (1999). These methods were developed for **1** extracted from *Brassica oleracea* var. *italica* (broccoli) which was available in a large amount and then applied to **1** isolated from *A. thaliana* and **1** produced by the *At1g65860* flavin monooxygenase in *A. thaliana* glucosinolate side chain. The three different samples of **1** were all shown to be epimerically pure and to possess the same stereochemistry.

Results

To determine the epimeric purity of **1** with respect to the sulfoxide group of its side chain, semi-synthetic **1** ($R_S S_S$–**1**, Fig. 2) was prepared as a reference by H_2O_2 oxidation of 4–methylthiobutylglucosinolate (**3**), which was isolated from *Eruca sativa* seeds (Fig. 2). Chiral chromatography and chiroptical methods failed to resolve the epimers. Chromatograms of semi–synthetic **1** after separation on a chiral column showed only a single compound, whose CD spectrum was indistinguishable from the spectrum of **1** isolated from broccoli, showing a plain curve centered near 230 nm. This absorption band was most probably due to the transitions of the chromophore belonging to the core glucosinolate structure, because it was also present in the CD spectrum of allyl glucosinolate, which does not contain a sulfoxide group. Turning to ^{1}H NMR, when **1** from *B. oleracea* and semi-synthetic **1** (racemic at the sulfoxide group) were analyzed in the presence of a chiral lanthanide shift reagent (CLSR), their spectra differed. In the ^{1}H NMR spectra of semi-synthetic **1**, the signal at δ 2.83 corresponding to the methyl–sulfoxide group was shown to consist of two non-equivalent signals (Fig. 2a). an HSQC experiment confirmed the phenomenon of non–equivalence demonstrating that the two sulfoxide ^{1}H signals were each correlated to a different ^{13}C signal with a different chemical shift (data not shown). In contrast, when **1** isolated from *B. oleracea* was analyzed using the same ^{1}H NMR conditions, the methyl sulfoxide signal at δ 2.85 did not show non–equivalence (Fig. 2b). Thus, **1** from *B. oleracea* was likely to be a pure epimer at the sulfoxide group. To confirm this epimeric purity determination, a sample was prepared mixing equimolar amounts of **1** from *B. oleracea* and semi–synthetic **1**. The ^{1}H NMR spectrum (Fig. 2c) showed an increase in the magnitude only for the downfield signal of the methyl sulfoxide and integration of the two signals gave a 3:1 ratio.
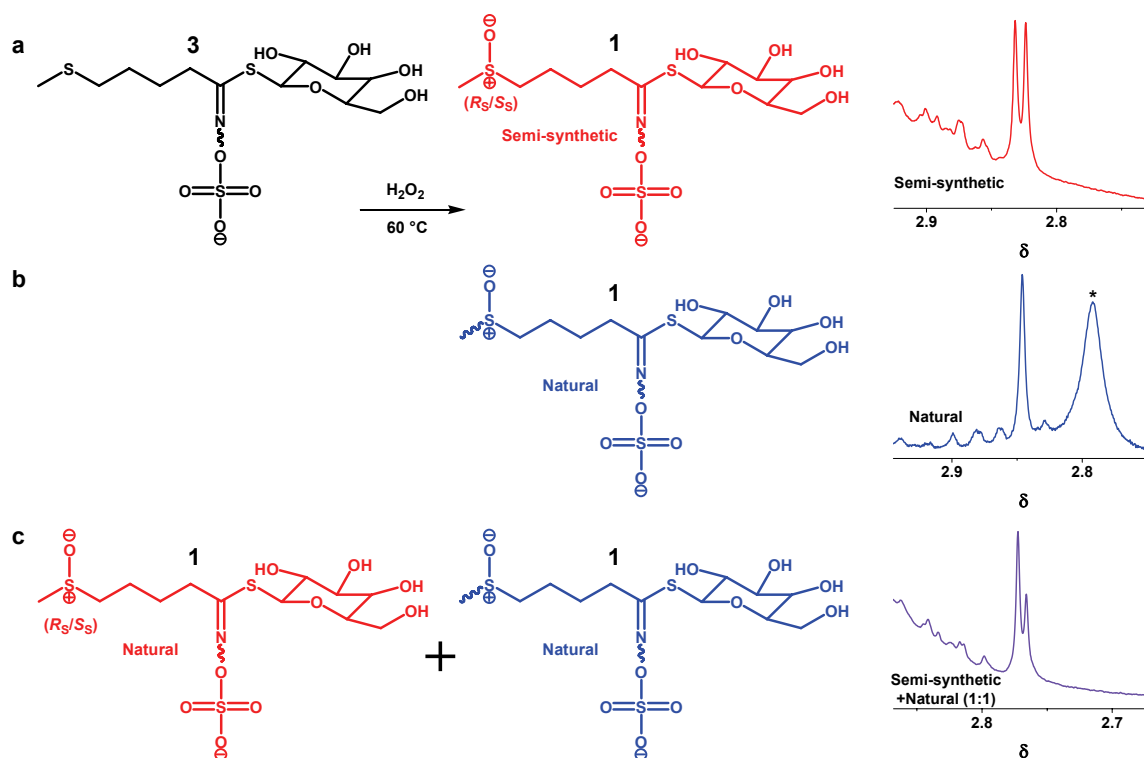
Figure 2. *Epimeric purity determination of 4–methylsulfinylbutylglucosinolate* (**1**) *from* Brassica oleracea *var.* italica *(broccoli) in relation to its sulfoxide group*. Compound **1** racemic with respect to its sulfoxide group [(1–R_S):(1–S_S), 50:50] was produced by symmetric oxidation of glucoerucin (**3**) with H_2O_2 for comparison of its methyl sulfoxide ^{1}H NMR signal (a) with that of **1** isolated from broccoli (b) in the presence of a chiral lanthanide shift reagent (CLSR). The signal at δ 2.9 in b (*) corresponds to HDO. To confirm the apparent epimeric purity of **1**, an equimolar mixture of semi-synthetic R_SS_S–**1** and **1** from broccoli was prepared. The resulting ^{1}H NMR spectrum (c) showed enhancement of the downfield signal only (ratio between signals = 3:1), indicating that **1** from broccoli is a pure epimer at the sulfoxide. The x axis has been shifted slightly to make the signals easier to compare. Slight differences in the chemical shift of the methyl sulfoxide protons are due to differences in the relative water contents of the samples. Spectra were recorded at 400 MHz in CD_3CN/CD_3OD (9:1) at 50 °C.

To determine the absolute configuration of the methyl sulfoxide group of **1** isolated from *B. oleracea*, the R_C– and S_C–*N*–(methoxyphenylacetyl)sulfoximine (*S*–*N*–MPA) derivatives (**4**, Fig. 3) were prepared (Yabuuchi et al., 1999). This method, in analogy to the Mosher method, takes advantage of chemical shift differences ($\Delta\delta = \delta S_C - \delta R_C$) between corresponding signals in the spectra of the diastereomeric R_C and S_C sulfoximine derivatives. Many chiral sulfoxides have been studied following this approach and a clear correlation between absolute configuration and ^{1}H NMR shift differences had been observed (Kusumi et al., 2006) when $CDCl_3$ was used as a NMR solvent. Unfortunately, the *S*–*N*–MPA derivatives of 4–methylsulfinylbutylglucosinolate (**4**) are insoluble in unpolar solvents such as $CDCl_3$ and C_6D_6, which are suitable for the elucidation of absolute configuration (Kusumi et al., 2006). Thus, we hydrolyzed **4** using myrosinase to produce an *S*–*N*–MPA derivative of sulforaphane (**5**, Fig. 3). The ^{1}H NMR signals in C_6D_6 of the methyl and four methylene groups of **5** showed chemical shift differences between the R_C and the S_C diastereoisomers. Unambiguous signal assignment for the two *S*–*N*–MPA diastereomers of **5** was carried out based on ^{1}H–^{1}H COSY and HSQC experiments. $\Delta\delta$ values for the methylene signals **I**, **II** and the methyl signal **V** were directly calculated from experimental ^{1}H NMR measurement, whereas $\Delta\delta$ for the methylene signals **III** and **IV** were calculated using δ values obtained from a computer simulation of the eight–spin system. Simulated δ values were as follows: **5**–S_C: **I** 2.27, **II** 0.63, **III** 1.02, **III'** 0.94, **IV** 2.52 and **IV'** 2.29 and for **5**-R_C: **I** 2.24, **II** 0.58, **III** 0.93, **IV** 2.50 and **IV'** 2.19. The chemical shift differences between the R_c and S_c sulfoximine derivatives of **5** are depicted at the bottom of Fig. 3 with the diameters of circles for each ^{1}H NMR signal proportional to $\Delta\delta$ magnitud and colors representing the sign of $\Delta\delta$ (Fig. 3). The sign of $\Delta\delta$ is the parameter that provides information about the configuration of the sulfoxide, because it is the result of the space–oriented aromatic shielding effect produced by the phenyl ring in MPA which selectively shields the methyl group (**V**) in the S_c configuration or the methylene protons (**I–IV**) in the R_c configuration. In the sulfoximine model, positive and negative $\Delta\delta$ lie on the left and right hand of the *N–S–O* plane, respectively (Kusumi et al., 2006). Because $\Delta\delta$ is negative for the methyl group and positive for the methylene protons in **5**, the absolute configuration of the sulfoxide in **5**, and by extension in **4** and **1** from *B. oleracea*, is inferred to be R_S. ^{1}H NMR analyses in the presence of CLSR were also performed on **1** extracted from *A. thaliana* rosette leaves and **1** produced by the *A.*

thaliana flavin monooxygenase expressed in *Escherichia coli* spheroplasts. In both cases, **1** was enantiomerically pure at the sulfoxide position and had an R_S absolute configuration (Fig. 4).
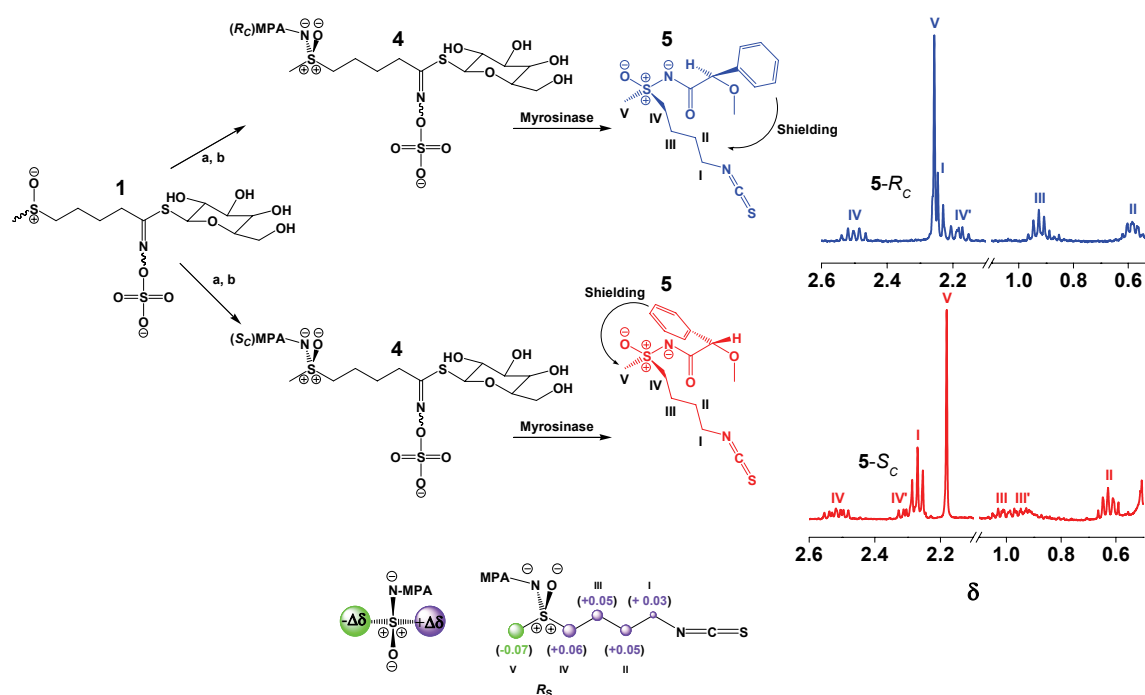
Figure 3. *Absolute configuration determination of the sulfoxide in 4-methylsulfinylbutylglucosinolate* (**1**) *by NMR using the sulfoximine method*. For solubility reasons, myrosinase *S–N–*MPA derivatives **5** were used instead of 4-methylsulfinylbutylglucosinolate *S–N–*MPA **4** for ^{1}H NMR analyses in C_6D_6. Comparison of δ values between the S_C and R_C diastereoisomers of *S-N*-MPA derivatives **5** resulted in chemical shift differences ($\Delta\delta = \delta S_C - \delta R_C$). The sign of $\Delta\delta$ was compared with the sulfoximine model at the bottom of the figure (Kusumi, 2006) and from these data the absolute configuration of the sulfoxide in **5**, and by inference in **1** and **2**, was determined as R_S. a: MSH, b: Coupling reagent; MPA: Methoxyphenylacetyl group. Structures of **5** are represented in an idealized perspective. Spectra recorded at 25 °C.

^{1}H NMR analyses in the presence of CLSR were also performed on **1** extracted from *A. thaliana* rosette leaves and **1** produced by the *A. thaliana* flavin monooxygenase expressed in *Escherichia coli* spheroplasts. In both cases, **1** was enantiomerically pure at the sulfoxide position and had an R_S absolute configuration (Fig. 4).
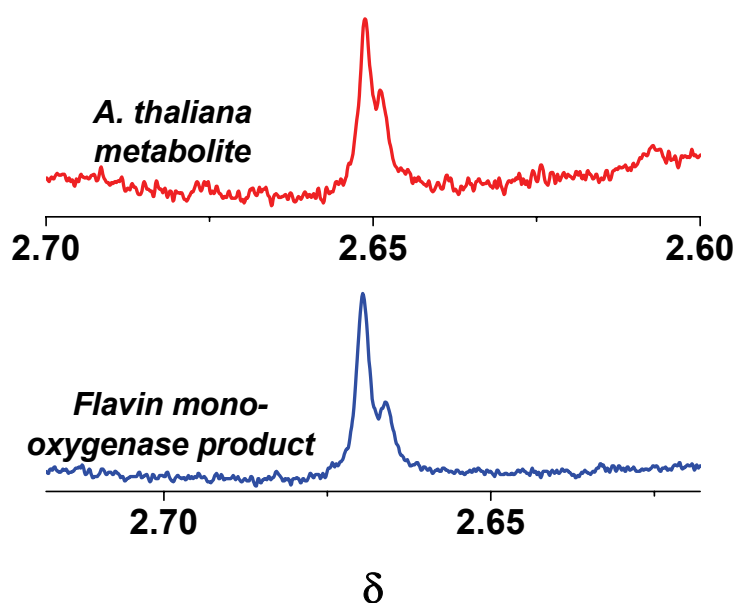

Figure 4. *Epimeric purity determination of 4–methylsulfinylbutylglucosinolate* (**1**) *isolated from* A. thaliana *and produced by* A. thaliana *flavin monooxygenase in relation to its sulfoxide group*. ^{1}H NMR spectra of equimolar mixtures of synthetic $R_S S_S$–**1** and **1** from *A. thaliana* showed enhancement of the downfield signal exclusively, as with **1** extracted from broccoli. Therefore, **1** is in both cases enantiomerically pure with an R_S absolute configuration. The *x*–axis has been shifted slightly to make the signals easier to compare. Slight differences in the chemical shift of the sulfoxide protons are due to differences in the relative water contents of the samples. Spectra were recorded at 50 °C.

Discussion

The asymmetric sulfoxide group of glucosinolate side chains creates a chiral center at an atom other than carbon due to its stable trigonal pyramidal geometry. Glucosinolate **1** isolated from *B. oleracea* var. *italica* and *A. thaliana* was epimerically pure with an R_s absolute configuration. This result is consistent with measurements of glucosinolate–derived isothiocyanates made by ORD over 40 years ago (Cheung et al., 1965). The product **1** of the *A. thaliana* flavin monooxygenase enzyme FMO$_{GS-OX1}$, reported to oxidize the methylthioether group of 4–methylthiobutylglucosinolate (**3**) to **1** has the same properties. These data suggest that the enzyme is stereospecific and support its involvement in glucosinolate side chain biosynthesis. Related enzymes may catalyze *S*–oxidation of methylthioalkyl glucosinolates throughout the Brassicaceae since a variety of different sulfoxide bearing isothiocyanates measured display levorotatory ORD spectra (Cheung et al., 1965), suggesting that the diverse sulfoxide bearing glucosinolate have the same R_S stereochemistry. The NMR methods used here for determining epimeric purity and absolute configuration have an advantage over the chiroptical spectroscopy previously used in that they can be applied directly on glucosinolates in a simple, reliable manner. Whether the absolute configuration of the side chain sulfoxide in glucosinolates or their hydrolysis products is important for biological activity in anticancer or plant–herbivore interactions, is still an open question. The methods developed in the present work should help to shed light on this topic and guide efforts to produce medically or agriculturally valuable glucosinolates by biotechnological or pure synthetic methods.

Experimental section

Extraction of glucosinolates

4–Methylsulfinylbutylglucosinolate (glucoraphanin, **1**) was isolated from broccoli seeds (*Brassica oleracea* L.; Juliwa Gemüse, Heidelberg, Germany), *Arabidopsis thaliana* Col–0 leaves grown in greenhouse facilities or *E. coli* spheroplast culture. 4–Methylthiobutylglucosinolate (glucoerucin, **3**) was isolated from *Eruca sativa* L. seeds (Saatzucht Quedlinburg, Germany) as described previously (Thies, 1988) with a final purification by HPLC (see method 1). Their structures were confirmed by electrospray LC–MS (method 1) using diagnostic ions detected in MS/MS mode (*m/z*: 436.0 [$M^{\ominus}$], 372, 259 for **1** and *m/z* 420.0 [$M^{\ominus}$], 340, 259, for **3**).

Synthesis of $R_S S_S$-4-methylsulfinylbutylglucosinolate ($R_S S_S$-1)

4–Methylthiobutylglucosinolate (**3**) (3 mg) was dissolved in H_2O (0.8 mL), H_2O_2 (0.03 mL) was added, and the mixture was heated at 60 °C for 30 min with agitation to afford **1** (Iori et al., 1999) which was then purified by preparative HPLC (method 1). The structure was confirmed by LC–MS using diagnostic ions in MS/MS mode (*m/z*: 436.0 [$M^{\ominus}$], 372, 259).

Synthesis of S_C– and R_C–N–(methoxyphenylacetyl)sulfoximine derivatives (4) of –4–methylsulfinylbutylglucosinolate

Synthesis of the sulfoximine derivatives of **1** isolated from broccoli followed the one–pot method described by Yabuuchi et al., (1999), with the following modifications: In the first step, DMF was used instead of CH_2Cl_2 as the solvent and *O*–mesitylsulfonylhydroxylamine (MSH) was produced as described by Krause (1971). The second reaction (condensation with methoxyphenylacetic acid) was carried out without modifications of the original procedure and the compound was purified by preparative HPLC (method 1). The structure of the products was confirmed by electrospray LC–MS (method 1) with diagnostic ions in MS/MS mode (*m/z*: 599.0 [$M^{\ominus}$], 436, 372, 259).

Enzymatic hydrolysis of *N*–(methoxyphenylacetyl)sulfoximine derivative 4 to 5

The S_C R_C sulfoxime derivatives **4** from broccoli were each dissolved in 500 µL of 100 mM Tricine (pH = 8.0). Myrosinase (2 mg) (Sigma, Germany) was added and the mixture stirred for 30 min at 25 °C. The structure of the *S*–*N*–MPA derivatives **5** obtained were confirmed by electrospray LC–MS (method 2) with diagnostic ions in MS/MS mode (*m/z*: 341.0 [*M*+H] $^{\oplus}$, 309, 281) and the products were purified using HPLC (method 2).

Assay of *A. thaliana* flavin monooxygenase

An expression construct containing the open reading frame of the FMO_{GS-OX1} line cloned into a pBAD–TOPO vector was cloned into *E. coli* and expressed as described (Hansen et al. 2007). An overnight culture (1 mL) started from single cell colony in LB (with 100 µg mL^{-1} ampicillin) was used to inoculate 100 mL of LB medium supplemented with 50 µg mL^{-1} carbicillin and the culture was grown at 37 °C to OD_{600}=0.5, at which time arabinose (final conc. 0.02%) was added. The culture was grown at 28 °C for 16 h and chilled on ice.

To isolate spheroplasts, the cells were centrifuged at 2,500 g for 10 min at 4 °C, and the pellet resuspended in 8.3 mL 0.2 M Tris/HCl (pH 7.6) using a soft brush. Then, 1.42 g sucrose, 16.7 µL 0.5 M EDTA, 41.7 µL PMSF (0.1M), 33.3 µL lysozyme (50 mg mL^{-1}), and 8.3 mL ice–cold water were added sequentially while slowly stirring. After an additional 30 min stirring at 4 °C, 166 µL 1 M cold MgOAc were added and the preparation centrifuged at 3,000 g for 10 min at 4 °C, and resuspended in 1.8 mL 10 mM Tris (pH 7.6) with 14 mM MgOAc and 60 mM KOAc. The suspension was homogenized in a pre-cooled Potter-Elvehjem glass homogenizer. Then 5 µL RNase (10 mg mL^{-1}) and 10 µL DNase (5mg mL^{-1}), were added and the mixture stirred for 30 min at 4 °C. After addition of 235 µL 87 % glycerol (to a total of 30 %), the spheroplasts were stored at -80 °C.

The assay was scaled up from that previously described (Hansen et al., 2007) to maximize product formation. An 0.5 mL volume of the spheroplast suspension was adjusted to 0.1 M Tricine buffer, pH 7.9, with 0.25 mM NADPH and 100 mM 4–metylthiobutylglucosinolate in a final volume of 1 mL. After an overnight incubation at room temperature, the products were extracted with 1 mL methanol and separated with HPLC method 1, as described below.

Circular dichroism

CD spectra were measured on a J-180 spectrometer (Jasco, Gross–Umstadt, Germany) with a 2 mm QS cuvette using MeOH as solvent. Spectra were recorded at 200–400 nm. Allyl glucosinolate used as a standard was purchased from Sigma.

High pressure liquid chromatography

All chromatographic analyses were carried out on an HPLC-1100 series equipment (Agilent Technologies, Böblingen, Germany) using different conditions. *Method 1*: Chromatograph was coupled to an Esquire 6000 ESI–Ion trap mass spectrometer (Bruker Daltonics, Hamburg, Germany) operated in negative mode in the range *m/z* 50–1000. Skimmer voltage, –40 eV; capillary exit voltage, –146.7 eV; capillary voltage, 4,000 V; nebulizer pressure, 35 psi; drying gas, 11 L min^{-1}; gas temperature, 330 °C. Elution was accomplished using an EC 250/4.6 Nucleodur Sphinx RP column (25 cm x 4.6 mm, 5 µm, Macherey–Nagel, Düren, Germany) coupled to a Supelguard^{TM} LC-18 precolumn (2 cm x 2.1 mm, Supelco, Taufkirchen, Germany) with a gradient of 0.2 % (v/v) formic acid (solvent A) and acetonitrile (solvent B) at a flow rate of 0.8 mL min^{-1} at 25 °C as follows: 0–100 % (v/v) B (15 min), 100 % B (3 min), 100–0 % (v/v) B (6 s), 0 % B (8 min 54 s). Eluent coming from the column was diverted in a ratio 4:1 before reaching the electrospray ionization unit. *Method 2*: Mass spectrometer operated in positive mode in the range *m/z* 30–500. Skimmer voltage, 40 eV; capillary exit voltage, 104.3 eV; capillary voltage, –4,000 V; nebulizer pressure, 35 psi; drying gas, 11 L min^{-1}; gas temperature, 300 °C. Elution: Supelcosil^{TM} LC–18 column (15 cm x 2.1 mm, 5 µm, Supelco) coupled to a Supelguard^{TM} LC–18 precolumn (2 cm x 2.1 mm, Supelco) with a gradient of 0.2 % (v/v) formic acid (solvent A) and acetonitrile (solvent B) at a flow rate of 0.25 mL min^{-1} at 25 °C as follows: 10–60 % (v/v) B (15 min), 60–100 % (v/v) B (6 s), 100 % B (1 min 54 s), 100–10 % (v/v) B (7 min 54 s). For isolation of compounds for NMR analysis chromatographic same conditions described in methods 1 and 2 were used but the column was connected to a fraction collector. *Method 3*: Chromatograph was connected to a UV detector operated at 230 nm. Elution was accomplished using a Chiralcel OD–H column (25 cm x 4.6 mm, 5 µm, Daicel) with methanol (isocratic) at a flow rate of 1 mL min^{-1} at 25 °C for 20 min.

Nuclear magnetic resonance spectroscopy

^{1}H NMR spectra were measured on an Avance 400 NMR spectrometer (Bruker Biospin, Rheinstetten, Germany) using a 5 mm BBI probe (^{1}H frequency 400.13 MHz) and on an Avance 500 NMR spectrometer (Bruker Biospin) equipped with a 5 mm TCI CryoProbe^{TM} (^{1}H frequency 500.13 MHz). Chemical shifts are given as δ values using TMS as a reference (internal standard). Tris[3–(heptafluoropropylhydroxymethylene)–d–camphorate]europium(III) (Eu(hfc)$_3$) was used as the chiral lanthanide shift reagent (CLSR) (Alfa, Germany). CDCl$_3$, CD$_3$CN, and CD$_3$OD were purchased from Deutero GmbH (Kastellaun, Germany) and C$_6$D$_6$ from Euriso–top GmbH (Saarbrücken, Germany). Spectra with the CLSR were recorded at 400 MHz in CD$_3$CN/CD$_3$OD (9:1) using a 1:5 molar ratio (**1**:CLSR) at 50 °C. Computer simulations of spectra were run with the ACD/C + ^{1}H NMR predictor software (ACD/Labs, Canada).

References

Bentley R. 2005. Role of sulfur chirality in the chemical processes of biology. *Chemical Society Reviews*, **34**: 609–624.

Carey F., Smith P., Maher R., Bryan R. 1976. An X-ray crystallographic structural study of sulfoxides derived from 2–phenyl–1,3–dithiane. *Journal of Organic Chemistry*, **42**: 961–967.

Cheung K., Kjær A., Sim G. 1965. The absolute configuration of sulphoxide mustard oils. *Chemical Communications*: 100–102.

Cho H., Plapp B. 1998. Specificity of alcohol dehydrogenases for sulfoxides. *Biochemistry*, **37**: 4482–4489.

Donnoli, M., Superchi S., Rosini C. 2006. Recent progress in application of spectroscopic methods for assigning absolute configuration of optically active sulfoxides. *Minireviews in Organic Chemistry*, **3**: 77–92.

Fahey J., Zalcmann A., Talalay P. 2001. The chemical diversity and distribution of glucosinolates and isothiocyanates among plants. *Phytochemistry*, **56**: 5–51.

Fimognari C., Hrelia P. 2007. Sulforaphane as a promising molecule for fighting cancer. *Mutation Research*, **635**: 90–104.

Halkier B., Gershenzon J. 2006. Biology and biochemistry of glucosinolates. *Annual Review in Plant Biology*, **57**: 303–33.

Hansen B., Kliebenstein D., Halkier B. 2007. Identification of a flavin-monooxygenase as the *S*-oxygenating enzyme in aliphatic glucosinolate biosynthesis in *Arabidopsis*. *The Plant Journal*, **50**: 902–910.

Iori R., Bernardi R., Gueyrard D., Rollin P., Palmieri S. 1999. *Bioorganic & Medicinal Chemistry Letters*, **9**: 1047–1048.

Kodama Y., Nishihata K., Nishio M. 1976. X–Ray study of ($\alpha S,SS/\alpha R,SR$)–1–(*p*-Bromophenyl)ethyl *t*–butyl sulphoxide and conformational analysis of diastereoisomeric pairs of 1–phenylethyl *t*–butyl sulphoxides. *Journal of the chemical society–Perkin Transactions* II, **13**: 1490–1495.

Krause J. 1971. *O*–Mesytylenesulfonylhydroxylamine. *Synthesis*, **3**: 140.

Kusumi T., Ooi T., Ohkubo Y., Yabuuchi T. 2006. The modified Mosher´s method and the sulfoximine method. *Bulletin of the Chemical Society of Japan*, **79**: 965–980.

Lherbet C., Keillor J. 2004. Probing the stereochemistry of the active site of gamma-glutamyl transpeptidase using sulfur derivatives of *L*–glutamic acid. *Organic & Biomolecular Chemistry*, **2**: 238–245.

Mislow K., Greenz M., Laur P., Chisholmz D. 1964. Optical rotatory dispersion and absolute configuration of dialkyl sulfoxides. *Journal of the American Chemical Society*, **87**: 665–666.

Olbe L., Carlsson E., Lindberg P. 2003. A proton–pump inhibitor expedition: The case histories of omeprazole and esomeprazole. *Nature Reviews Drug Discovery*, **2**: 132–139.

Thies W. 1988. Isolation of sinigrin and glucotropaeolin from cruciferous seeds. *FETT Wissenschaft Technologie–Fat Science Technology*, **90**: 311–314.

Yabuuchi T., Kusumi T. 1999. NMR Spectroscopic determination of the absolute configuration of chiral sulfoxides via *N*–(Methoxyphenylacetyl)sulfoximines. *Journal of the American Chemical Society*, **121**: 10646–10647.

Zhang Y., Tang L. 2007. Discovery and development of sulforaphane as a cancer chemopreventive phytochemical. *Acta Pharmacologica Sinica*, **28**: 1343–1354.

3. General Discussion

The glucosinolate–myrosinase system of the Brassicales represents an effective chemical barrier for minimizing herbivory of many consumers of these plant species. Yet, some herbivores have the ability to successfully use Brassicales as a food source. In metabolic terms, this ability relies on the presence of biochemical processes that can prevent the formation of noxious glucosinolate hydrolysis products. One of these processes is the desulfation of glucosinolates via sulfatase activity, because desulfated glucosinolates are no longer hydrolysable by myrosinases. This mechanism is expressed by the Brassicales specialist *Plutella xylostella*[5] (the diamondback moth) as well as by the generalists *Helix pomatia*[6] (the roman or edible snail) and *Schistocerca gregaria*[3] (the desert locust). It is interesting to note that, although these herbivores display contrasting feeding habits (monophagy *vs*. polyphagy), they both make use of the same mechanism to avoid the noxious effects of glucosinolate hydrolysis products. This means that some generalist herbivores might not necessarily be less adapted to feed on protected plants in comparison to specialist herbivores. In other words, it might well be that evolution has produced some generalist herbivores able to exploit a broad range of hosts as a result of a very efficient detoxifying metabolism capable of dealing with many classes of toxic plant metabolites.

Another mechanism to avoid the formation of noxious glucosinolate hydrolysis products is the expression of proteins that influence the hydrolysis reaction mechanism, leading to the production of compounds presumably less toxic. This is the mechanism employed by the Brassicales specialist *Pieris rapae*, which produces a protein, NSP, that influences the hydrolysis of glucosinolates leading to the production of nitriles instead of isothiocyanates. However, some nitriles produced by NSP activity might not be completely harmless to *P. rapae*. For example, the research in this thesis showed that NSP converts benzylglucosinolate into phenylacetonitrile upon digestion, but unlike other nitriles phenylacetonitrile is further metabolized, undergoing conjugation with an amino acid. It appears likely that lipophilic aromatic compounds such as phenylacetonitrile represent a threat to larval physiology; therefore, *P. rapae* has developed the ability to bind them with amino acids, making them water soluble and easily excretable with the feces.

These results demonstrate how complex the metabolic machinery of insect herbivores may have to be in order to neutralize the chemical defences of plant they feed on. In this case, *P. rapae* may have to use a more complex detoxification system than *P. xylostella*, also a Brassicales specialist in order to convert all glucosinolates to nitriles and then further process certain nitriles. Animal detoxification systems are generally thought to impose costs because of the resources used in construction and maintenance of the enzymes and supply of the cofactors; for this reason, possession of a detoxification system must give some evolutionary advantage. If insect herbivores lacking detoxification mechanisms cannot efficiently use Brassicales as host plants, those insects having this trait may exploit an ecological niche not available for other herbivores, reducing the amount of competition. Interestingly, larvae of *P. rapae* perform better than *P. xylostella* larvae when feeding on the benzylglucosinolate–accumulating *T. majus*, with shorter growing rates and bigger pupation size (Francisco Badenes, Pers. Comm.). These data suggest that the extra cost of the multienzymatic detoxification system expressed by *P. rapae* is compensated for by making its caterpillars better competitors when exploiting plants containing benzylglucosinolate.

Generalists as well as specialist herbivores are represented in almost every single ecosystem. This suggests that being a specialist is not always the best option for the prevailing conditions. The dilemma of the specialist is that its survival is tied to the presence of one or a few host species which may not always be abundant. From this perspective, generalists have the advantage in not being so dependent on a limited group of plants. On the other hand, it is likely an insurmountable challenge for many generalists to circumvent the great variety of different plant toxins likely to be encountered in a single location. This seems to be the case for *Heliothis armigera*, an insect herbivore classified as a generalist, whose larvae have been recorded on a broad range of hosts, including members of the Brassicales[4]. However, the performance of *H. armigera* on glucosinolate–myrosinase containing plants is rather poor. In work performed for here, there was no indication that this species has detoxification systems acting on glucosinolates or their hydrolysis products. When larvae were offered two genotypes of *A. thaliana*, the wild–type Col–0 and the *tgg1–tgg2* mutant, the latter unable to hydrolyze glucosinolates, larvae performed significantly better on *tgg1–tgg2* plants, suggesting that they are negatively affected by glucosinolate hydrolysis products in their diet. These results

corroborate previous reports showing the efficiency of the glucosinolate–myrosinase system in reducing the herbivory exerted by some insect species on plants of the Brassicales.

Curiously, the early larval stages of *H. armigera* displayed a different feeding behavior depending on whether they were reared on *A. thaliana* Col–0 or *tgg1–tgg2* plants. In the first case, the larvae tended to feed only on an area located between the midvein and the edge of the leaf, at the center of the leaf lamina. The fine scale distribution of foliar glucosinolates determined by MALDI–imaging showed that these defenses tend to be more concentrated towards the midvein and the leaf periphery, coinciding with the leaf areas avoided by *H. armigera* larvae. These findings offer insight into plant-herbivore interactions at a new spatial scale. The differential distribution of plant metabolites in various organs is a common plant feature, for instance in *A. thaliana*[2]. According to the optimal defense theory those plant tissues or organs with high fitness value will be better defended[1]. Thus, inter–organ variation in defensive metabolite content might reflect the energetic cost associated with the biosynthesis and/or translocation of defensive compounds. If only a limited amount of resources can be invested in producing and/or moving plant defensive metabolites, locating them in tissues with a high fitness or a high risk of herbivory might be an evolutionary stable strategy to resist herbivore attack. This argument can be extended to the intra–organ level as well. If there are sites in an organ with a higher prevalence of herbivory or higher fitness value, selection might have acted in favoring individuals concentrating defensive compounds on these areas. In the case of the glucosinolate–myrosinase system the biosynthesis of aliphatic glucosinolates involves about ten enzymatic reactions and a supply of amino acids, acetyl–CoA, glucose, NADPH and other cofactors. If the demands of other plant processes limit the amount of glucosinolates that can be produced, these defenses may be preferentially deployed to those areas that have greater value to the plant and/or are at higher risk of suffering herbivory. Independent of being generalists or specialists, many chewing insect herbivores tend to start ingesting leaves from the periphery. As an example, *P. rapae* displays this pattern when feeding on Brassicales (scheme 4). This feeding behavior might be the ecological cause of the uneven foliar distribution of glucosinolates in *A. thaliana*, and the preferential distribution of glucosinolates in the periphery might function as a barrier to insect feeding.

Scheme 4. Feeding behavior of late instars of *P. rapae*. *P. rapae* 4th–5th instar exemplify a typical insect feeding pattern, where leaf consumption starts at the edge. This might be the reason why glucosinolates tend to be more concentrated towards the leaf periphery. Assuming that their biosynthesis is energetically demanding, concentrating chemical defenses at a site at high risk of attack site might be a better strategy than distributing them evenly throughout an organ.

As a model organism, *A. thaliana* is one of the most studied plant species, yet many aspects of its biology remain unexplored, especially its ecological interactions. At present, the combination of ecological studies with our in depth knowledge of *A. thaliana* biochemistry and physiology provides strong evidence for the biological function of glucosinolates. It seems that the primary, if not sole biological role of these metabolites is as defenses. But, interestingly, no research has been performed aimed to identify the molecular basis of their biological activity. Experimental evidence strongly supports the idea that glucosinolates are effective as chemical barriers against some non–specialized herbivores, but their mode of action remains unknown. Thus, I have begun a pharmacologically–oriented research program focused on revealing the molecular basis of glucosinolates and/or their hydrolysis products. The strategy involves the synthesis of labeled analogues of glucosinolates for determining their absorption, distribution, metabolism ad excretion after being ingested by a susceptible insect herbivores. *H. armigera* was chosen as a model system considering that is a generalist herbivore capable of feeding on Brassicales

species but experiences negative effects attributable to glucosinolates hydrolysis products.

For tracking the metabolism of any kind of xenobiotic it is desirable to use a molecular probe that resembles as closely as possible the parental compound. 4–methylsulfinylbutylglucosinolate was selected as the chief molecule to be studied because it is the major glucosinolate in *A. thaliana* Col–0 leaves as well as in the crops cabbage and broccoli, which are occasionally used by *H. armigera* as hosts in nature (Shudong Liu, pers. comm.).   The hydrolysis product of 4–methylsulfinylbutylgluosinolate, sulforaphane, is a chiral molecule due to the presence of an asymmetric sulfoxide group.   Chirality is often a crucial structural feature of compounds in biology, determining whether a molecule is active or not. For this reason, I investigated the epimeric composition and the absolute stereochemistry of 4–methylsulfinylbutylglucosinolate extracted from plants.   NMR experiments demonstrated that the compound present in plants is a pure epimer with the R_S absolute configuration. Hence, any molecular probe developed for tracking its metabolism in *H. armigera* should reproduce the stereochemical properties of the parental glucosinolate.

Shedding light on the mode of action of glucosinolates against susceptible insect herbivores will provide a new perspective on the ecological interactions between Brassicales and their herbivores, allowing the evaluation of ecological patterns at molecular level.   Knowing what cells and biochemical processes are affected by glucosinolate hydrolysis products should permit a better understanding of the structural diversity of this family of plant metabolites, because different glucosinolate hydrolysis products might affect different cells or biochemical pathways depending on the nature of the herbivore. On the other hand this knowledge will also provide a more precise understanding of the evolution of specialization displayed by some herbivores consuming Brassicales. Information about the mode of action of these compounds makes it possible to study the evolution of those traits that led to adaptation to a glucosinolate containing diet. A precise description of the mode of action of glucosinolate hydrolysis products is not only relevant in basic research, but also could contribute to crop protection. The long term development of insect herbivores sensitive to glucosinolate hydrolysis products might be used for biological control by being released in areas where insects have become a pest.   If the released, sensitive strain can effectively mate with the established population, the

off–spring maybe unable to feed on glucosinolate–myrosinase containing plants. Alternatively, knowledge of the mode of action of glucosinolates could be used to design new selective pesticides, such as inhibitors of specific glucosinolate-detoxifying enzymes.

Biology is more than solely chemistry, but understanding the chemistry of life is absolutely essential to comprehend the complexity of physiology and ecology of living things. Chemical ecology pursues this aim and studies like this provide information regarding the role of specific plant metabolites as regulators of ecological interaction with insect herbivores. Further investigation of the glucosinolate-myrosinase system and herbivore counteradaptations should reveal much more about the ecology and evolution of plant-insect interactions.

References

[1]Barto K., Cipollini D. 2005. Testing the Optimal Defense Theory and the Growth–Differentiation Balance Hypothesis in *Arabidopsis thaliana*. *Oecologia*, 146: 169–178.

[2]Brown P., Tokuhisa J., Reichelt M., Gershenzon J. 2003. Variation of Glucosinolate Accumulation Among Different Organs and Developmental Stages of *Arabidopsis thaliana*. *Phytochemistry*, 62(3): 471–481.

[3]Falk K., Gershenzon J. 2007. The Desert Locust, *Schistocerca gregaria*, Detoxifies the Glucosinolates of *Schouwia purpurea* by Desulfation. *Journal of Chemical Ecology*, 33: 1542–1555.

[4]Firempong S., Zalucki M. 1989. Host Plant Preferences of Populations of Helicoverpa–Armigera (Hubner) (Lepidoptera, Noctuidae) From Different Geographic Locations. *Australian Journal of Zoology*, 37(6): 665–673.

[5]Ratzka A., Vogel H., Kliebenstein D., Mitchell–Olds T., Kroymann J. 2002. *Proc. Natl. Acad. Sci. USA*, 99, 11223–11 228.

[6]Thies W. 1979. Detection and Utilization of a Glucosinolate Sulfohydrolase in the Edible Snail, *Helix pomatia*. *Naturwissenschaften*, 66: 364–365.

4. Conclusion

Brassicales plants experience different rates of herbivory depending upon the degree of specialization of the herbivore trying to feed on them. Specialist herbivores, like *P. rapae*, have developed an effective detoxifying system directed to prevent the formation of noxious glucosinolate derivatives. However, some of the initial detoxification products may still exert significant toxicity. This makes it necessary for *P. rapae* larvae to perform additional chemical modifications in order to completely cancel out the negative effects associated with a glucosinolate–myrosinase containing diet. On the other hand, the presence of glucosinolate hydrolysis products effectively deters the feeding activity of the early larval stages of the generalist insect *H. armigera* and in the long term impacts the growth rate of the caterpillars. *H. armigera* larvae feeding on glucosinolate-containing tissue act to minimize their intake of these defensive compounds suggesting that they lack the metabolic machinery necessary for the effective metabolism of glucosinolate hydrolysis products.

The differential ability displayed by some insects to exploit Brassicales plants as food sources thus appears to depend on the presence or absence of metabolic adaptations which enable them to avoid or minimize the negative effects caused by the glucosinolate hydrolysis products. On the other hand, the distribution of glucosinolates in plant tissue appears to have been selected to maximize its defensive value to the plant itself. Hence glucosinolates or, more precisely, their hydrolysis products have a major role in regulating ecological interactions between herbivores and the plants producing them.

5. Zusammenfassung

Trotz ihrer chemischen Abwehr mittels Glukosinolaten werden Pflanzen der Familie der Brassicaceaen von unterschiedlichen Herbivoren gefressen. Die sogennanten Spezialisten wie *Pieris rapae*, die nur Glukosinolat–haltige Pflanzen fressen, haben offensichtlich effektive Systeme für die Entgiftung der Glukosinolate entwickelt. Untersuchungen zu diesem Phänomen hatten gezeigt, dass *P. rapae* ein Protein (NSP) besitzt, welches die Hydrolyse der Glukosinolate beeinflusst, wodurch die Glukosinolate zu Nitrilen anstatt zu Isothiocyanaten abgebaut werden. Die Toxizität der Nitrile ist vermutlich geringer als die der Isothiocyanate, wodurch *P. rapae* Brassicaceae–Pflanzen fressen kann. Allerdings könnten bestimmte Nitrile selbst giftig sein, und es wurde hier gezeigt, dass das aus Benzylglukosinolat produzierte Nitril (Phenylacetonitril) bei *P. rapae* mit einer Aminosäure konjugiert wird. Das Konjugat ist polarer als das Nitril, und *P. rapae* kann es leichter ausscheiden. Das zeigt, dass die Aktivität des NSP nicht in jedem Falle zur Bildung von für das Insekt unschädlichen Verbindungen führt. Andererseits wurde bei dem Generalisten *Helicoverpa armigera* gezeigt, dass die Hydrolyseprodukte von Glukosinolaten seine Fressaktivität reduzieren können. Wenn die Raupen gezwungen wurden, sich ausschließlich von Blättern der glukosinolathaltigen *Arabidopsis thaliana* zu ernähren, fraßen sie nur auf den Teilen des Blattes mit geringer Konzentration an Glukosinolaten. Es ist zu vermuten, dass den jungen Larvalstadien von *H. armigera* Raupen die notwendige metabolische Ausrüstung zur Entgiftung der Hydrolyseprodukte von Glukosinolaten fehlt oder dass sie nur über kleine Mengen dieser schützenden Enzyme und Kofaktoren verfügen.

Die Fähigkeit der Herbivoren an chemisch verteidigten Pflanzen zu fressen, wird einerseits den metabolischen Adaptationen wie Entgiftung, Ausscheidung oder Desensibilisierung des Zielproteins zugeschrieben, andererseits sensorischen Anpassungen, die die Raupen benutzen, um die Pflanzen zu lokalisieren und als Wirtspflanzen zu akzeptieren. Die Ergebnisse dieser Doktorarbeit stützen die Theorie, dass metabolische Adaptationen die Auswahl der Wirtspflanzen von Herbivoren bestimmen. Dabei wird deutlich gezeigt, dass das Ernährungsverhalten von Insekten, die Brassicaceae–Pflanzen fressen, entscheidend von ihrer Fähigkeit abhängt, Glukosinolat-Abbauprodukte zu entgiften.

7. Acknowledgements

I wish to express my deep thankfulness to all the people who love me, those who always showed me their friendship and camaraderie; life has been much more enjoyable because of you. I wish also to thank all the people who share and taught me important things in life: Love, friendship, wisdom, solidarity, honesty, perseverance, gratitude, tolerance, respect, justice, hardworking, football. I am who I am in part because of you. I want to thank particularly to all the people who helped me to achieve successfully the biggest academic objective of my life so far, obtaining my Ph. D. degree. Scientists, students, technicians and administrative co-workers are equally acknowledged. Whenever our paths cross in the future, you know well you will have a friend in me.

8. Curriculum Vitae

Personal Data

Name: Luis Fredd Leonardo Vergara Montalvo

Date of birth: November 6th 1976

Place of birth: Otumba, Estado de México, México

Nacionality: Mexican

Address: Jansonstr. 6 07745, Jena

e-mail: fvergara@ice.mpg.de, fredd@servidor.unam.mx

Education

2005–present: Graduate student at the Max–Planck–Institut für chemische Ökologie and the Friedrich–Schiller–Universität, Jena.

2002–2004: Master in chemistry at the National and Autonomous University of Mexico (UNAM), Mexico City.

1997–2001: Bachelor in biology at the National and Autonomous University of Mexico (UNAM), Mexico City.

Research Experience

2001. Royal Botanic Gardens, Kew, Wakehurst Place, England.

2003. Higher Council of Scientific Research, Madrid, Spain.

Publications

Vergara F., Svatoš A., Schneider B., Reichelt M., Gershenzon J., and Wittstock U. 2006. Glycine Conjugates in a Lepidopteran Insect Herbivore–The Metabolism of Benzylglucosinolate in the Cabbage White Butterfly, *Pieris rapae*. *Chembiochem* 7(12): 1982–1989.

Shroff R.*, Vergara F.*, Muck A., Svatoš A., and Gershenzon J. 2008. Nonuniform Distribution of Glucosinolates in *Arabidopsis thaliana* Leaves has Important Consequences for Plant Defense. *Proceedings of the National Academy of Sciencies of United States* 105(16): 6196–2601. *These two authors have equally contributed to this work.

Vergara F.[1]*, Wenzler M.[1]*, Hansen B.[2], Kliebenstein D.[3], Halkier B.[2], Gershenzon J.[1], and Schneider B.[1]. Determination ofthe Absolute Configuration of the Glucosinolate Methyl Sulfoxide Group Reveals a Stereospecific Biosynthesis of the Side Chain. *Phytochemistry* 69(15): 2737-2742. *These two authors have equally contributed to this work.

9. Selbständigkeitserklärung

Entsprechend der Promotionsordnung der Biologisch–Pharmazeutischen Fakultät der Friedrich–Schiller–Universität erkläre ich, dass ich vorliegende Arbeit selbständig und nur unter Verwendung der angegebenen Hilfsmittel und Bibliographie angefertig habe.

Personen, die an der Durchführung und Auswertung des Materials und bei der Herstellung der Manuskripte beteiligt waren, sind am Beginn der Arbeit und jedes Manuskripts angegeben.

Die Hilfe eines Promotionsberaters wurde nicht in Anspruch genommen.

Die vorgelegte Arbeit wurde weder an der Friedrich–Schiller–Universität Jena noch an einer anderen Hochschule als Dissertation eingereicht.

Fredd Vergara